

# Two-Photon Absorption Properties of Proquinoidal D-A-D and A-D-A Quadrupolar Chromophores

Kimihiro Susumu,<sup>†,‡</sup> Jonathan A. N. Fisher,<sup>§,||</sup> Jieru Zheng,<sup>⊥</sup> David N. Beratan,<sup>\*,⊥,◇,♦</sup>  
Arjun G. Yodh,<sup>\*,§</sup> and Michael J. Therien<sup>\*,⊥</sup>

Departments of <sup>†</sup>Chemistry and <sup>§</sup>Physics and Astronomy, University of Pennsylvania, Philadelphia, Pennsylvania 19104-6323, United States

Departments of <sup>◇</sup>Biochemistry, <sup>♦</sup>Physics, and <sup>⊥</sup>Chemistry, Duke University, Durham, North Carolina 27708, United States

 Supporting Information

**ABSTRACT:** We report the synthesis, one- and two-photon absorption spectroscopy, fluorescence, and electrochemical properties of a series of quadrupolar molecules that feature proquinoidal  $\pi$ -aromatic acceptors. These quadrupolar molecules possess either donor–acceptor–donor (D-A-D) or acceptor–donor–acceptor (A-D-A) electronic motifs, and feature 4-*N,N*-dihexylaminophenyl, 4-dodecyloxyphenyl, 4-(*N,N*-dihexylamino)benzo[*c*][1,2,5]thiadiazolyl or 2,5-dioctyloxyphenyl electron donor moieties and benzo[*c*][1,2,5]thiadiazole (BTD) or 6,7-bis(3',7'-dimethyloctyl)[1,2,5]thiadiazolo[3,4-*g*]quinoxaline (TDQ) electron acceptor units. These conjugated structures are highly emissive in nonpolar solvents and exhibit large spectral red-shifts of their respective lowest energy absorption bands relative to analogous reference compounds that incorporate phenylene components in place of BTD and TDQ moieties. BTD-based D-A-D and A-D-A chromophores exhibit increasing fluorescence emission red-shifts, and a concomitant decrease of the fluorescence quantum yield ( $\Phi_f$ ) with increasing solvent polarity; these data indicate that electronic excitation augments benzothiadiazole electron density via an internal charge transfer mechanism. The BTD- and TDQ-containing structures exhibit blue-shifted two-photon absorption (TPA) spectra relative to their corresponding one-photon absorption (OPA) spectra, and display high TPA cross sections ( $>100$  GM) within these spectral windows. D-A-D and A-D-A structures that feature more extensive conjugation within this series of compounds exhibit larger TPA cross sections consistent with computational simulation. Factors governing TPA properties of these quadrupolar chromophores are discussed within the context of a three-state model.



## INTRODUCTION

Two-photon absorption (TPA) is the basis for an increasing number of optical and electro-optical applications that include data storage,<sup>1–3</sup> three-dimensional microfabrication,<sup>4–6</sup> biological imaging,<sup>7–12</sup> optical limiting,<sup>13–16</sup> and photodynamic therapy.<sup>17–21</sup> The potential of these technologies, in turn, continues to drive development of materials with improved TPA properties. For example, TPA-enhanced materials boost absorption efficiency at low excitation intensity and, therefore, help minimize damage due to laser irradiation. Therefore, an improved understanding of chromophoric structural factors that may be manipulated to improve TPA will undoubtedly impact a variety of technologies that depend upon this nonlinear optical (NLO) property.

To date, a number of design strategies for materials with large TPA cross sections ( $\delta$ ) have been proposed and demonstrated. D- $\pi$ -D, D-A-D, and A-D-A structural motifs, where D,  $\pi$ , and A refer, respectively, to electron donor,  $\pi$ -conjugated bridge, and electron acceptor units, have been shown to exhibit exceptionally large TPA cross sections for many D,  $\pi$ , and A moieties.<sup>22–34</sup> Quadrupolar structures, in particular, have experimentally<sup>28</sup> and theoretically<sup>35,36</sup> demonstrated enhanced TPA cross sections that are approximately

an order of magnitude greater than those of dipolar analogues. In addition, quadrupolar compounds have higher fluorescence quantum yields relative to corresponding dipolar compounds, most likely due to cancellation of D–A dipoles which otherwise would tend to induce charge transfer quenching of fluorescence; such augmented fluorescence quantum yields are useful, for example, in imaging technologies that rely on TPA.<sup>22,24,28</sup> Corresponding octopolar chromophores,<sup>37–42</sup> as well as multibranched conjugated systems that include dendrimers,<sup>43–48</sup> can also provide materials with high TPA cross sections.

Incorporation of proquinoid structures, such as benzothiadiazole and thiadiazoloquinoxaline, into the main chain of  $\pi$ -conjugated oligomers and polymers is an established means to diminish optical and potentiometric band gaps.<sup>49–58</sup>  $\pi$ -Conjugated materials that feature benzothiadiazole or thiadiazoloquinoxaline units have been exploited as both emissive and charge transport functional elements for organic light-emitting diodes<sup>54,55,59–63</sup> and as key components of photovoltaic cells<sup>60,64–73</sup> and field effect transistors.<sup>59,74–76</sup> Because

**Received:** January 4, 2011

**Revised:** March 24, 2011

**Published:** May 13, 2011

proquinoidal units function as electron accepting moieties in structures having extended conjugation, D-A-D- and A-D-A-type chromophores that take advantage of benzothiadiazole or thiadiazoloquinoxaline building blocks might be expected to exhibit enhanced TPA properties.

In this paper, we report the synthesis, one- and two-photon absorption spectroscopy, fluorescence, and electrochemical properties of a series of quadrupolar molecules that feature benzothiadiazole or thiadiazoloquinoxaline  $\pi$ -aromatic acceptors and compute the one- and two-photon absorption spectra for these species, to provide further insight into the origins of the one-photon absorption (OPA) and TPA properties that derive from the presence of the proquinoidal units.

## EXPERIMENTAL SECTION

**Materials.** Manipulations were carried out under argon previously passed through an O<sub>2</sub> scrubbing tower (Schweitzerhall R3-11 catalyst) and a drying tower (Linde 3-Å molecular sieves), unless otherwise stated. Air-sensitive solids were handled in a Braun 150-M glovebox. Standard Schlenk techniques were employed to manipulate air-sensitive solutions. Tetrahydrofuran (THF) was distilled from K/4-benzoylbiphenyl under N<sub>2</sub>. Triethylamine, MeOH, and CH<sub>2</sub>Cl<sub>2</sub> were distilled from CaH<sub>2</sub> under N<sub>2</sub>. Pyridine was also dried over CaH<sub>2</sub> and distilled under reduced pressure. The catalysts Pd(PPh<sub>3</sub>)<sub>4</sub>, tris(dibenzylideneacetone)dipalladium(0) (Pd<sub>2</sub>dba<sub>3</sub>), Pd(PhCN)<sub>2</sub>Cl<sub>2</sub>, triphenylarsine (AsPh<sub>3</sub>) and P(*t*-Bu)<sub>3</sub> (10 wt % solution in hexanes) were purchased from Strem Chemicals and used as received. 4-Bromobenzo[c][1,2,5]thiadiazole,<sup>77</sup> 4,7-dibromobenzo[c][1,2,5]thiadiazole,<sup>77</sup> 5,6-diamino-4,7-dibromobenzo[c][1,2,5]thiadiazole,<sup>78</sup> 4,7-bis[(trimethylsilyl)ethynyl]benzo[c][1,2,5]thiadiazole,<sup>56</sup> and 4,7-diiodobenzo[c][1,2,5]thiadiazole<sup>79</sup> were prepared by literature methods. All NMR solvents were used as received. The supporting electrolyte used in the electrochemical experiments, tetra-*n*-butylammonium hexafluorophosphate, was recrystallized twice from ethanol and dried under vacuum at 70 °C overnight prior to use. All the other chemicals were used as received.

Chemical shifts for <sup>1</sup>H NMR spectra are relative to the tetramethylsilane (TMS) signal in deuterated solvent (TMS,  $\delta$  = 0.00 ppm). All *J* values are reported in Hertz. Flash and size exclusion column chromatographic separations were performed on the benchtop, using respectively silica gel (EM Science, 230–400 mesh) and Bio-Rad Bio-Beads SX-1 as media. CI mass spectra were acquired at the Mass Spectrometry Center at the University of Pennsylvania. MALDI-TOF mass spectroscopic data were obtained with a PerSeptive Biosystems Voyager–DE RP; samples for these experiments were prepared as micromolar solutions in THF; dithranol (Aldrich) was utilized as the matrix.

**Instrumentation.** <sup>1</sup>H NMR spectra were recorded on 360 MHz DMX-360, 300 MHz DMX-300, or 250 MHz AC-250 Bruker spectrometers. Electronic absorption spectra were recorded on a Shimadzu PharmaSpec UV1700 spectrophotometer. Fluorescence spectra were obtained with a Spex Fluorolog-3 spectrophotometer (Jobin Yvon Inc., Edison, NJ) that utilized a PMT detector. These fluorescence spectra were corrected using the spectral output of a calibrated light source supplied by the National Bureau of Standards. Fluorescence quantum yields were measured in argon-purged solutions at room temperature. Quinine sulfate in 1.0 N H<sub>2</sub>SO<sub>4</sub> ( $\Phi_f$  = 0.55)<sup>80</sup> and rhodamine 101 inner salt in EtOH ( $\Phi_f$  = 1.00)<sup>81</sup> were used as standards. Time-correlated single-photon counting (TCSPC) experiments that measured fluorescence lifetimes were carried out using an

Edinburgh Analytical Instruments FL/FS 900 spectrometer, using either a nanosecond flash lamp operating under an atmosphere of H<sub>2</sub> gas (0.50–0.55 bar, 1.2 ns full width at half-maximum (fwhm), 40 kHz repetition rate) or a blue (450 ± 15 nm) light-emitting diode (Picoquant PLS 450/PDL 800-B) triggered at a frequency of 100 kHz by a Berkeley Nucleonics 555 pulse generator, as excitation sources.<sup>82,83</sup> This diode produced light pulses of 450 ps fwhm with a power of 15  $\mu$ W. TCSPC data were analyzed by iterative convolution of the fluorescence decay profile with the instrument response function using software provided by Edinburgh Instruments.

Cyclic voltammetric measurements were carried out on an EG&G Princeton Applied Research model 273A Potentiostat/Galvanostat. The electrochemical cell for these experiments utilized a platinum disk working electrode, a platinum wire counter-electrode, and a saturated calomel reference electrode (SCE). The reference electrode was separated from the bulk solution by a junction bridge filled with the corresponding solvent/supporting electrolyte solution. The ferrocene/ferrocenium redox couple was utilized as an internal potentiometric standard.

**Two-Photon Absorption Spectra.** The background theory and a detailed experimental description of our TPA spectra measurements were described previously.<sup>84,85</sup> The samples were dissolved in toluene at a concentration of 3.8–10.5  $\times 10^{-5}$  M. The sample cells were degassed by freeze–pump–thaw methods (three cycles) and filled with argon gas. Throughout our experiments, we used a 100  $\mu$ M solution of fluorescein in H<sub>2</sub>O (pH  $\sim$  13) as a standard calibration sample. We assume herein that the one-photon and two-photon fluorescence quantum yields of fluorescein are equal and that the fluorescence quantum yield is constant over the spectral range of the experiment.

**Computational Studies.** We used time-dependent density-functional theory (TDDFT) within the collective electronic oscillator (CEO) framework recently described by Tretiak et al.<sup>86</sup> to calculate one- and two-photon absorption spectra for this series of quadrupolar proquinoid compounds. In our implementation of the CEO framework, frequency-dependent polarizabilities are described by functions that can be obtained from response theory, including corresponding functional derivatives up to third order in the driving field.<sup>87</sup> Briefly, the procedure for computing frequency-dependent polarizabilities using TDDFT involved: (1) computing the ground-state density matrix, (2) obtaining a set of transition densities and frequencies (for coupled harmonic oscillators), (3) calculating anharmonicity tensors, and (4) summing over states for the desired response. This method was found to be efficient computationally and accurate for calculating nonlinear polarizabilities of large D–A substituted conjugated molecules.<sup>86,88,89</sup> The method typically performs better than semiempirical methods (such as ZINDO and PM3 methods) and other common ab initio approaches (such as CI singles and time-dependent Hartree–Fock methods) for describing molecular excited states and electronic excitation energies.<sup>90,91</sup>

All electronic structure and nonlinear response calculations were carried out using the GAUSSIAN 98<sup>92</sup> and CEO programs,<sup>93</sup> while geometry optimization was performed using the Hartree–Fock (HF) method with a 6-31G basis set. In order to maximize computational efficiency, the solubilizing substituents of these proquinoidal chromophores (*N,N*-dihexylamino, dodecyloxy, octyloxy and 3,7-dimethyloctyl groups) were replaced by structurally simpler analogues (*N,N*-dimethylamino, methoxy, and methyl groups, respectively). All molecular geometries were optimized beginning with planar structures with symmetry constraints. The excitation energies, dipole matrices, and Coulomb- and

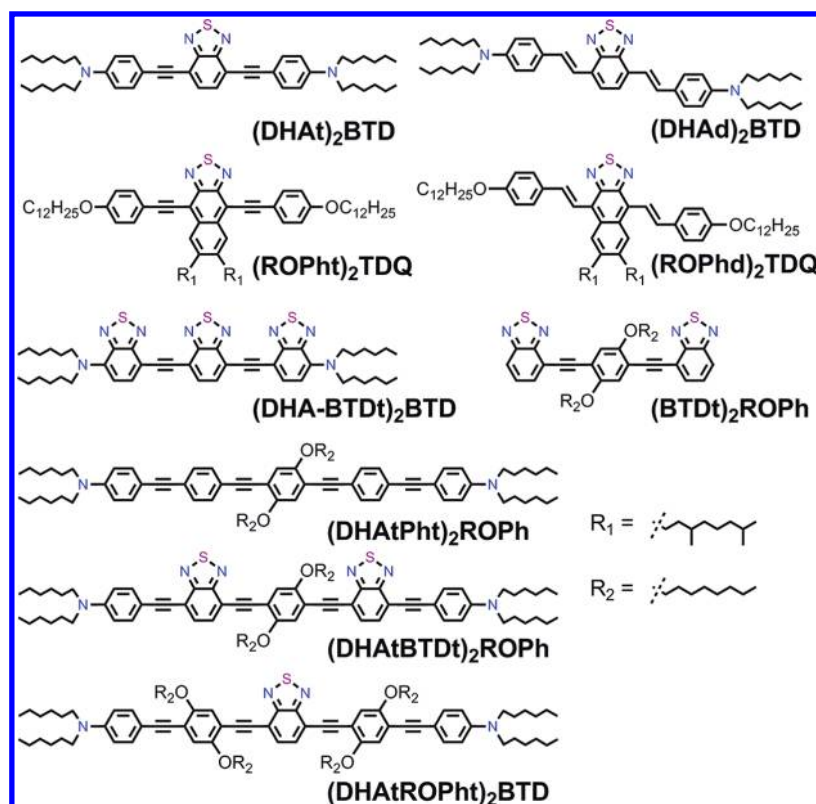


**Figure 1.** Structures of D-A-D and A-D-A chromophores, along with their respective abbreviations; note that **t** and **d** signify connectivities utilizing respectively C–C triple and double bonds.

exchange-interaction matrices were calculated using the TDDFT method in GAUSSIAN 98 with a 6-31G basis set and the B3LYP functional. The energies and corresponding transition densities of the first 10 singlet excited states were calculated. We did not include more excited states in the calculation because it has been reported that increasing the number of excited states from 6 to 30 changes the resulting cross section by only about 10%.<sup>86,89</sup> The CEO program was used to compute first-, second-, and third-order responses based on electronic structure analysis from GAUSSIAN 98.<sup>93</sup> These simulations neglected solvation effects. An empirical damping factor  $\Gamma = 0.1$  eV (obtained from experimental studies of phenylene-vinylene derivatives) was used.<sup>22,24</sup>

**Synthesis and Characterization.** A full account of the synthesis and characterization of all new compounds, complete with tabulated spectral data, is provided in the Supporting Information (SI).

## RESULTS AND DISCUSSION

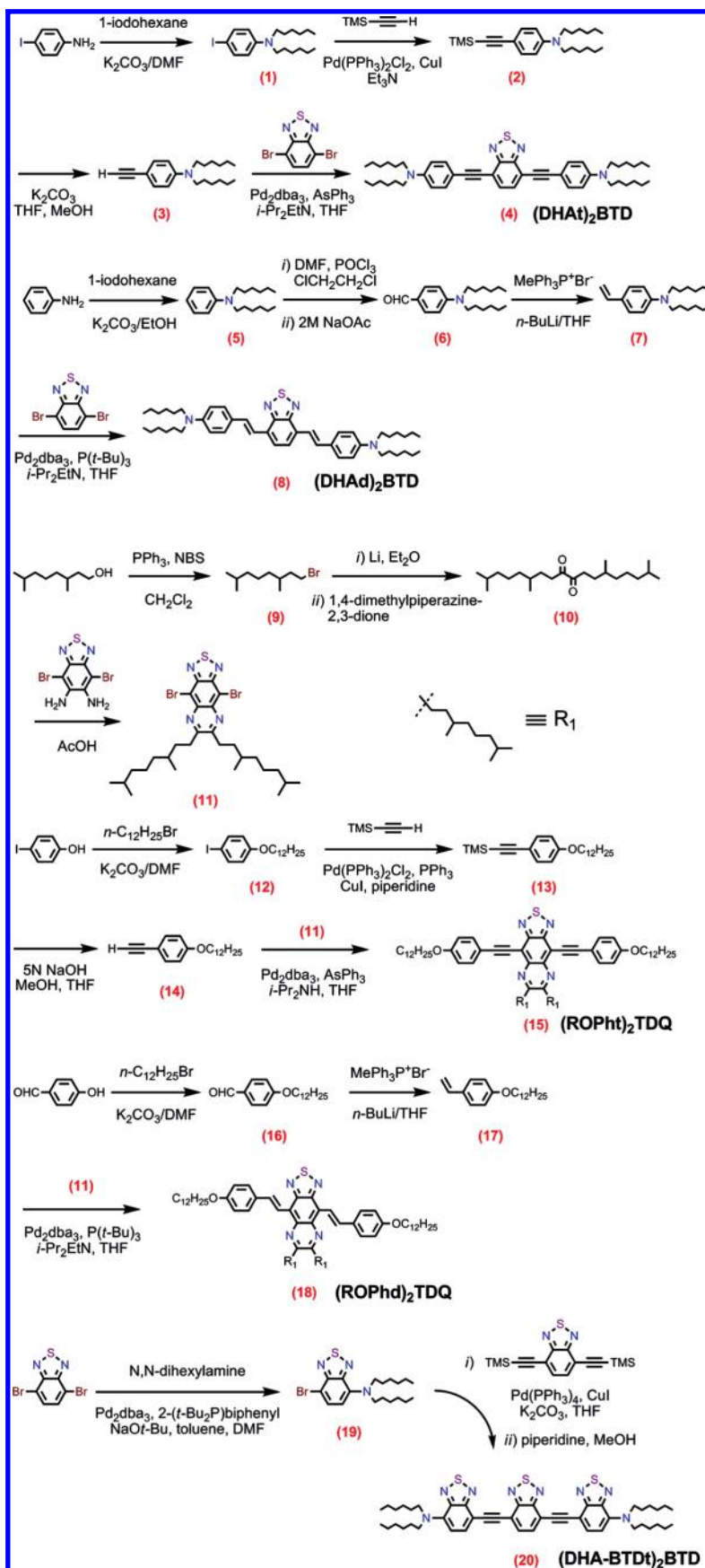
**Synthesis.** Structures of D-A-D and A-D-A chromophores examined in this study are shown in Figure 1; these molecules were synthesized by Pd-mediated cross-coupling reactions involving substituted aromatic donor and proquinoidal acceptor building blocks (Scheme 1; see Supporting Information for details). Benzo[*c*][1,2,5]thiadiazole (BTD) and 6,7-bis(3',7'-dimethyloctyl)[1,2,5]thiadiazolo[3,4-*g*]quinoxaline (TDQ) were selected as proquinoidal spacer units. For the thiadiazoloquinoxaline-containing structures, note that 3,7-dimethyloctyl groups serve as 6- and 7-TDQ-ring substituents, which facilitate solubility of these large planar molecules.

Proquinoidal BTD and TDQ units have been used to drive enhanced conjugation in semiconducting oligomers and polymers, and as electron acceptor moieties;<sup>49,51,56,94</sup> these units play a similar role in the Figure 1 chromophores. For these D-A-D and A-D-A structures, aromatic units are connected by either ethyne or ethene linkers, through respective Sonogashira or Heck coupling reactions. These simple, efficient coupling protocols enabled facile synthesis of the Figure 1 compounds (Supporting Information).

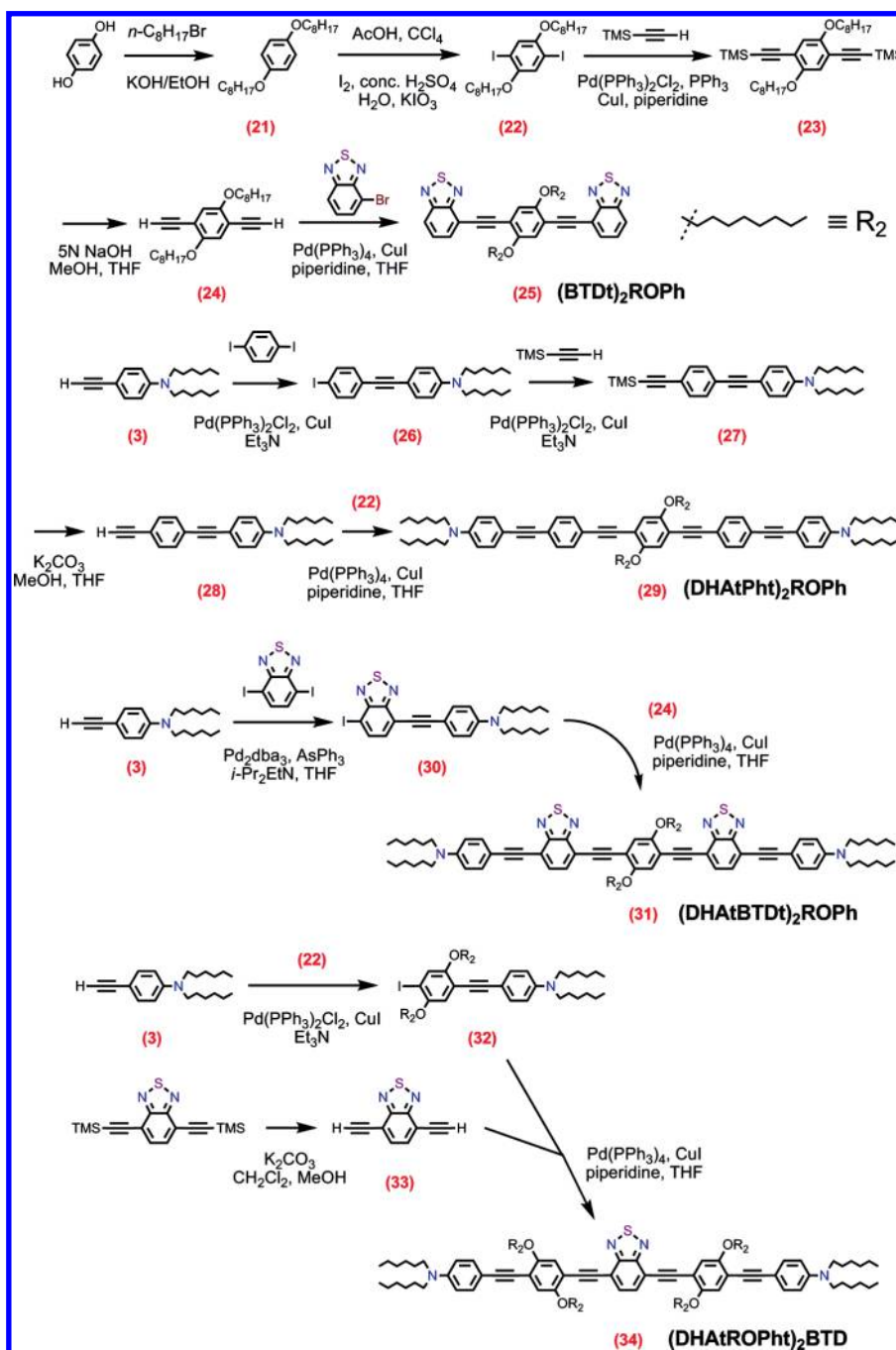
**One-Photon Absorption Spectra.** The linear (one-photon) electronic absorption spectra of the proquinoidal D-A-D and A-D-A molecules, measured in solvents of varying dielectric constant, are displayed in Figure 2. Fluorescence and comparative one-photon absorptive extinction coefficient data acquired in toluene solvent are compiled in Table 1. As highlighted in the Figure 2 spectral data, these chromophores feature excellent solubility in a wide range of solvents, and underscore the chromophoric impact of the proquinoidal components. Notice, for example, that the lowest absorption maxima of (DHAt)<sub>2</sub>BTD and (DHAd)<sub>2</sub>BTD are, respectively, 111 nm (5681 cm<sup>−1</sup>) and 131 nm (5929 cm<sup>−1</sup>) red-shifted relative to their corresponding reference compounds featuring phenylene spacers (1,4-bis[(4'-*N,N*-dimethylaminophenyl)ethyn-1'-yl]benzene<sup>95</sup> and 1,4-bis[(4'-*N,N*-di-*n*-butylaminophenyl)ethen-1'-yl]benzene).<sup>24</sup> (ROPh)<sub>2</sub>TDQ and (ROPhd)<sub>2</sub>TDQ express similar magnitude spectroscopic red-shifts (10392 cm<sup>−1</sup> (toluene) and ~9500 cm<sup>−1</sup> (CH<sub>2</sub>Cl<sub>2</sub>)) of their respective lowest energy absorption maxima, relative to analogous 1,4-bis[(4'-methoxyphenyl)ethyn-1'-yl]benzene<sup>95</sup> and 1,4-bis[(4'-*n*-butoxyphenyl)ethen-1'-yl]benzene<sup>96</sup> spectroscopic benchmarks.



Scheme 1. Synthetic Routes to D-A-D and A-D-A Chromophores and Their Precursors



Scheme 1. Continued



For systems with identical donor and acceptor units, compounds featuring ethene-based connectivity manifest more substantial low energy absorption band spectroscopic red-shifts relative to corresponding compounds in which ethynyl moieties link aromatic units [ $\lambda_{\text{max}}((\text{DHAt})_2\text{BTD, toluene}) = 501 \text{ nm} < \lambda_{\text{max}}((\text{DHAd})_2\text{BTD, toluene}) = 540 \text{ nm}$ ;  $\lambda_{\text{max}}((\text{ROPhT})_2\text{TDQ, toluene}) = 562 \text{ nm} < \lambda_{\text{max}}((\text{ROPhd})_2\text{TDQ, toluene}) = 626 \text{ nm}$ ]. While all of these D-A-D and A-D-A chromophores evince only modest solvatochromism of their respective lowest energy absorption band maximum (Figure 2), (DHAt)<sub>2</sub>BTD, (DHAd)<sub>2</sub>BTD, (DHA-BTDt)<sub>2</sub>BTD, (DHAtPhT)<sub>2</sub>ROPh, (DHAtBTDt)<sub>2</sub>ROPh, and (DHAtROPhT)<sub>2</sub>BTD exhibit

systematic red-shifts in their absorption edges with increasing solvent polarity. Note that (ROPhT)<sub>2</sub>TDQ, (ROPhd)<sub>2</sub>TDQ, and (BTDt)<sub>2</sub>ROPh do not display similar red-shifts of their long wavelength absorption band edges with increasing solvent polarity, consistent with the diminished electron-releasing character of alkoxyphenyl (ROPh) relative to the dialkylaminophenyl group.

**Fluorescence Spectra.** In contrast to the linear absorption spectroscopic data, the fluorescence spectra of these proquinoidal D-A-D and A-D-A compounds show a clear dependence on solvent dielectric constant (Figure 3). As the solvent polarity increases, the

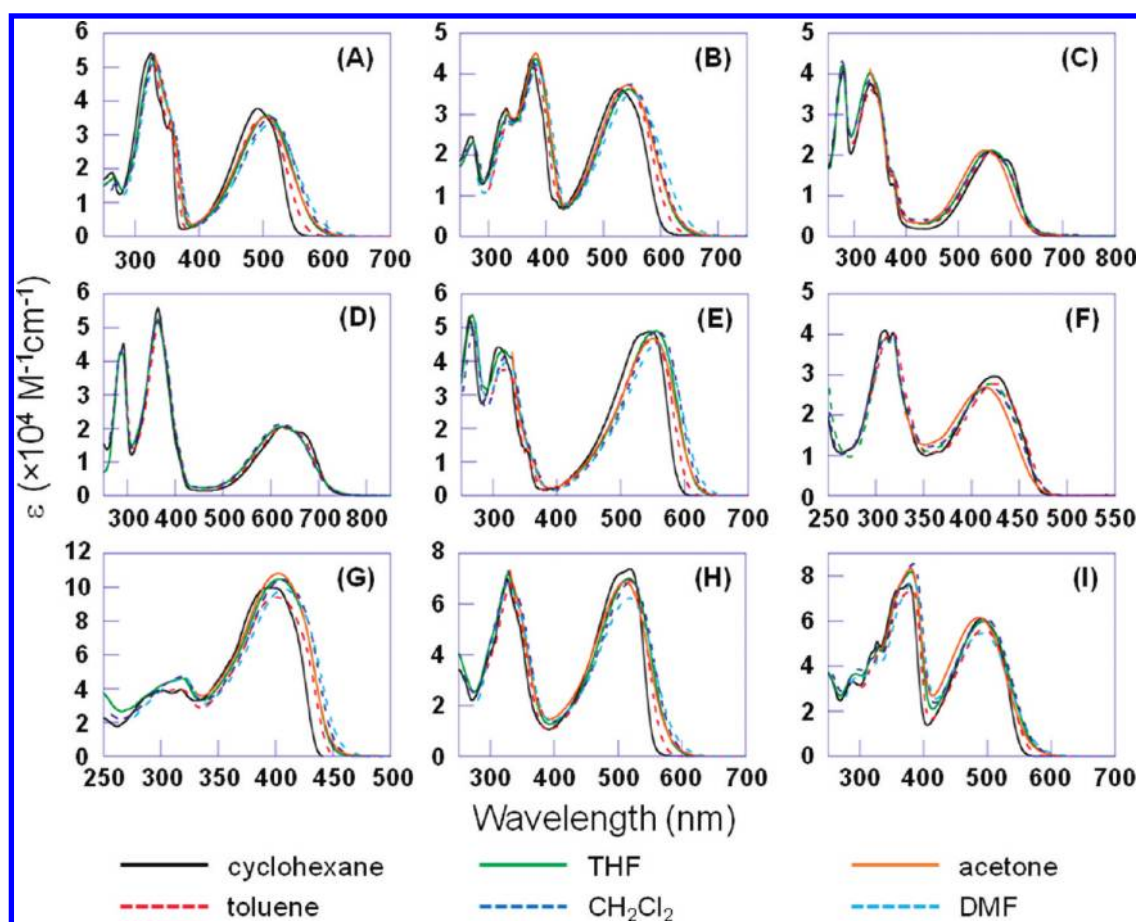


**Figure 2.** Electronic absorption spectra of (A) (DHAt)<sub>2</sub>BTD, (B) (DHAd)<sub>2</sub>BTD, (C) (ROPht)<sub>2</sub>TDQ, (D) (ROPhd)<sub>2</sub>TDQ, (E) (DHA-BTDt)<sub>2</sub>BTD, (F) (BTDt)<sub>2</sub>ROPh, (G) (DHAtPhT)<sub>2</sub>ROPh, (H) (DHAtBTDt)<sub>2</sub>ROPh, and (I) (DHAtROPhT)<sub>2</sub>BTD, recorded in cyclohexane, toluene, tetrahydrofuran (THF), CH<sub>2</sub>Cl<sub>2</sub>, acetone, and dimethylformamide (DMF) solvents.

**Table 1.** Lowest Energy Linear Absorption Band Maxima, Extinction Coefficients, and Fluorescence Maxima of Proquinoidal (DHAt)<sub>2</sub>BTD, (DHAd)<sub>2</sub>BTD, (ROPht)<sub>2</sub>TDQ, (ROPhd)<sub>2</sub>TDQ, (DHA-BTDt)<sub>2</sub>BTD, (BTDt)<sub>2</sub>ROPh, (DHAtPhT)<sub>2</sub>ROPh, (DHAtBTDt)<sub>2</sub>ROPh, and (DHAtROPhT)<sub>2</sub>BTD Chromophores Determined in Toluene Solvent

	linear absorption			fluorescence emission	
	$\lambda_{\text{abs}}$ (nm)	$\nu$ (cm <sup>-1</sup> )	$\epsilon$ ( $\times 10^4$ M <sup>-1</sup> cm <sup>-1</sup> )	$\lambda_{\text{em}}$ (nm)	$\nu$ (cm <sup>-1</sup> )
(DHAt) <sub>2</sub> BTD	501	19960	3.53	598	16722
(DHAd) <sub>2</sub> BTD	540	18519	3.70	651	15361
(ROPht) <sub>2</sub> TDQ	562	17794	2.04	655	15267
(ROPhd) <sub>2</sub> TDQ	626	15974	2.01	727	13755
(DHA-BTDt) <sub>2</sub> BTD	549	18215	4.61	612	16340
(BTDt) <sub>2</sub> ROPh	424	23585	2.77	501	19960
(DHAtPhT) <sub>2</sub> ROPh	401	24938	9.41	445	22472
(DHAtBTDt) <sub>2</sub> ROPh	515	19417	6.96	590	16949
(DHAtROPhT) <sub>2</sub> BTD	494	20243	5.64	587	17036

fluorescence maxima red-shift and the corresponding fluorescence quantum yield decreases (Table 2). Identical spectroscopic trends have been observed in other D-A-D and A-D-A systems and have been attributed to an S<sub>1</sub> → S<sub>0</sub> electronic transition having internal charge transfer (ICT) character.<sup>39,44,97</sup> For the chromophores featuring dialkylamino electron releasing groups, substantial solvent-dependent Stokes shifts are observed [(DHAt)<sub>2</sub>BTD (2176 (cyclohexane), 4918 (DMF) cm<sup>-1</sup>); (DHAd)<sub>2</sub>BTD (2410 (cyclohexane), 4260 (DMF) cm<sup>-1</sup>); (DHA-BTDt)<sub>2</sub>BTD (1279 (cyclohexane), 2985 (DMF) cm<sup>-1</sup>); (DHAtPhT)<sub>2</sub>ROPh (2158

(cyclohexane), 7209 (DMF) cm<sup>-1</sup>); (DHAtBTDt)<sub>2</sub>ROPh (1123 (cyclohexane), 5243 (acetone) cm<sup>-1</sup>); (DHAtROPhT)<sub>2</sub>BTD (2316 (cyclohexane), 5688 (CH<sub>2</sub>Cl<sub>2</sub>) cm<sup>-1</sup>)] at the other extreme lie the (ROPht)<sub>2</sub>TDQ and (ROPhd)<sub>2</sub>TDQ chromophores, which evince only modest solvent-dependent Stokes shifts [(ROPht)<sub>2</sub>TDQ (2046 (cyclohexane), 3068 (acetone) cm<sup>-1</sup>); (ROPhd)<sub>2</sub>TDQ (1969 (cyclohexane), 2468 (CH<sub>2</sub>Cl<sub>2</sub>) cm<sup>-1</sup>)], suggesting a diminished degree of ICT character to their respective S<sub>0</sub> → S<sub>1</sub> and S<sub>1</sub> → S<sub>0</sub> electronic transitions.

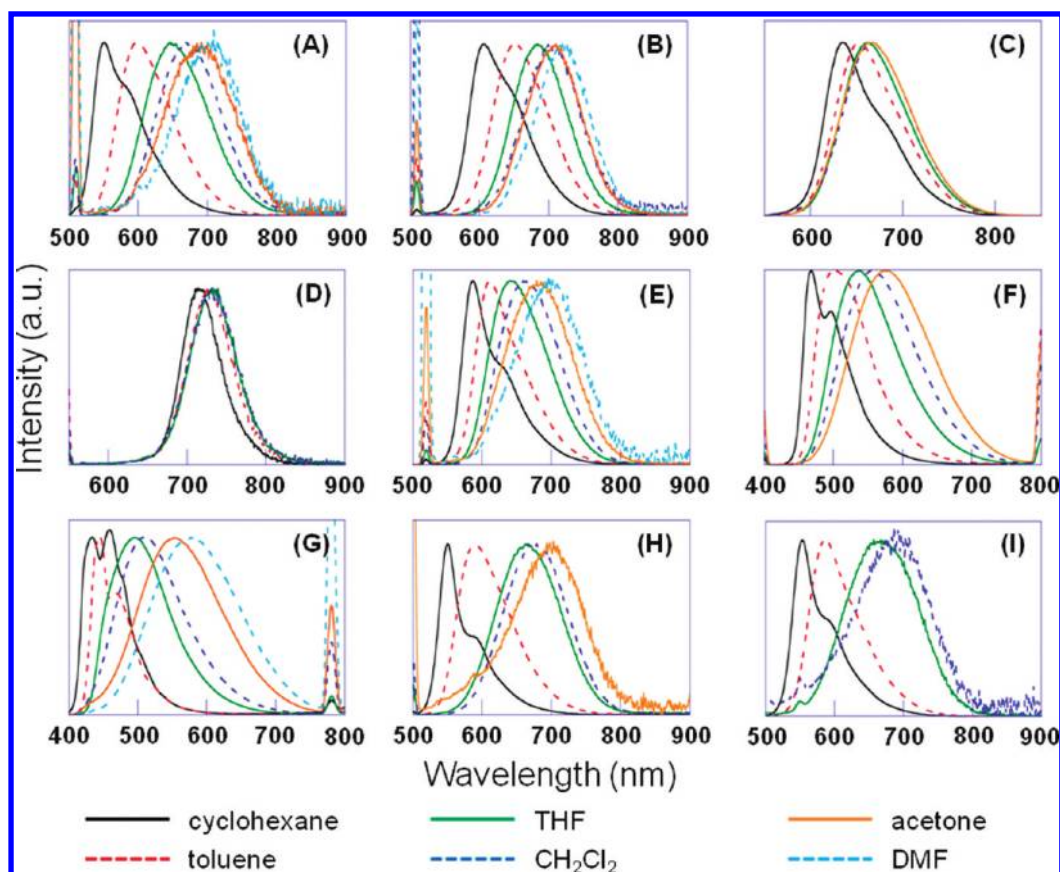


Figure 3. Fluorescence spectra of (A) (DHAt)<sub>2</sub>BDT, (B) (DHAd)<sub>2</sub>BDT, (C) (ROPh)<sub>2</sub>TDQ, (D) (ROPhd)<sub>2</sub>TDQ, (E) (DHA-BTDt)<sub>2</sub>BDT, (F) (BTDt)<sub>2</sub>ROPh, (G) (DHAtPh)<sub>2</sub>ROPh, (H) (DHAtBTDt)<sub>2</sub>ROPh, and (I) (DHAtROPh)<sub>2</sub>BDT, recorded in cyclohexane, toluene, THF, CH<sub>2</sub>Cl<sub>2</sub>, acetone, and DMF solvents. Sharp peaks evident at ~500 and 800 nm derived from scattered light from the excitation source.

Table 2. Fluorescence Quantum Yields of Proquinoidal D-A-D and A-D-A Chromophores Determined in Cyclohexane, Toluene, THF, CH<sub>2</sub>Cl<sub>2</sub>, Acetone, and DMF Solvents

	cyclohexane	toluene	THF	CH <sub>2</sub> Cl <sub>2</sub>	acetone	DMF
(DHAt) <sub>2</sub> BDT	0.87	0.84	0.31	0.25	0.011	0.0031
(DHAd) <sub>2</sub> BDT	0.75	0.42	0.13	0.037	0.031	0.0083
(ROPh) <sub>2</sub> TDQ	0.48	0.42	0.27	0.27	0.25	
(ROPhd) <sub>2</sub> TDQ	0.054	0.034	0.017	0.013		
(DHA-BTDt) <sub>2</sub> BDT	0.13	0.088	0.11	0.095	0.014	0.0034
(BTDt) <sub>2</sub> ROPh	0.59	0.66	0.48	0.37	0.15	
(DHAtPh) <sub>2</sub> ROPh	0.86	0.89	0.88	0.78	0.35	0.13
(DHAtBTDt) <sub>2</sub> ROPh	0.65	0.80	0.14	0.080	0.0012	<0.001
(DHAtROPh) <sub>2</sub> BDT	0.59	0.56	0.0097	0.0013	<0.001	<0.001

Solvent-polarity-dependent fluorescence spectra can be interpreted in terms of the Lippert equation (eq 1), which expresses the magnitude of the Stokes shift in terms of changes in the molecular dipole moment that occur concomitantly with electronic excitation.

$$\tilde{\nu}_a - \tilde{\nu}_f = \left[ \frac{\epsilon - 1}{2\epsilon + 1} - \frac{n^2 - 1}{2n^2 + 1} \right] \frac{2(\mu_E - \mu_G)^2}{hca^3} + \text{constant} \quad (1)$$

Here  $\tilde{\nu}_a$  and  $\tilde{\nu}_f$  are the respective peak absorption and emission energies expressed in wavenumbers,  $\epsilon$  is the dielectric constant,  $n$  is the refractive index of the solvent,  $\mu_E$  and  $\mu_G$  correspond, respectively, to the magnitudes of the excited- and ground-state dipole

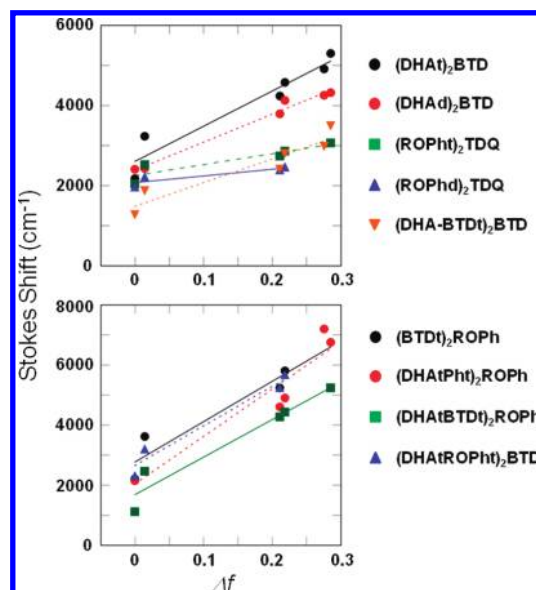
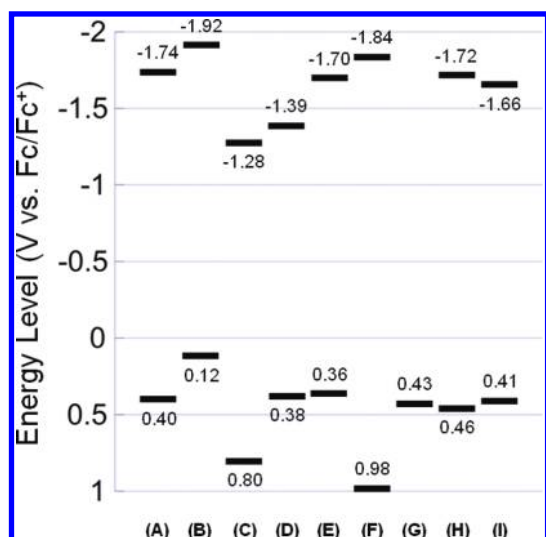


Figure 4. Lippert plots determined for the (DHAt)<sub>2</sub>BDT, (DHAd)<sub>2</sub>BDT, (ROPh)<sub>2</sub>TDQ, (ROPhd)<sub>2</sub>TDQ, (DHA-BTDt)<sub>2</sub>BDT, (BTDt)<sub>2</sub>ROPh, (DHAtPh)<sub>2</sub>ROPh, (DHAtBTDt)<sub>2</sub>ROPh, and (DHAtROPh)<sub>2</sub>BDT chromophores.

moments,  $h$  is Planck's constant,  $c$  is the speed of light, and  $a$  is the radius of the solute spherical cavity.





**Figure 5.** Potentiometrically determined  $E_{1/2}^{0/+}$  and  $E_{1/2}^{-/0}$  values measured in  $\text{CH}_2\text{Cl}_2$  solvent for (A) (DHAt)<sub>2</sub>BTD, (B) (DHAd)<sub>2</sub>BTD, (C) (ROPh<sub>t</sub>)<sub>2</sub>TDQ, (D) (ROPh<sub>d</sub>)<sub>2</sub>TDQ, (E) (DHA-BTDt)<sub>2</sub>BTD, (F) (BTDt)<sub>2</sub>ROPh, (G) (DHAtPh<sub>t</sub>)<sub>2</sub>ROPh, (H) (DHAtBTDt)<sub>2</sub>ROPh, and (I) (DHAtROPh<sub>t</sub>)<sub>2</sub>BTD. Experimental conditions are described in Table 3. Redox potentials shown are relative to the ferrocene/ferrocenium ( $\text{Fc}/\text{Fc}^+$ ) redox couple, which was used as an internal standard in these experiments.

The bracketed term in eq 1 is often referred to as the orientational polarizability ( $\Delta f$ ; eq 2).

$$\Delta f = \frac{\epsilon - 1}{2\epsilon + 1} - \frac{n^2 - 1}{2n^2 + 1} \quad (2)$$

Plots of the magnitude of the Stokes shift ( $\tilde{\nu}_a - \tilde{\nu}_f$ ) versus the orientational polarizability are displayed in Figure 4. This analysis highlights the fact that the slopes of the Lippert plots for the TDQ-containing chromophores are smaller than those of the D-A-D and A-D-A structures that are based on the BTD unit. This result likely derives from (i) the reduced electron-releasing character of alkoxyphenyl relative to the dialkylaminophenyl group, which leads to smaller magnitude  $\mu_E - \mu_G$  values and (ii) the fact that TDQ possesses a larger solute spherical cavity radius relative to BTD. Likewise, it is interesting that the observed Lippert plot slopes for the longer (DHAtBTDt)<sub>2</sub>ROPh and (DHAtROPh<sub>t</sub>)<sub>2</sub>BTD molecules are similar in magnitude to the slope for the shorter (BTDt)<sub>2</sub>ROPh chromophore; this effect is consistent with the expectation that while (DHAtBTDt)<sub>2</sub>ROPh and (DHAtROPh<sub>t</sub>)<sub>2</sub>BTD should possess larger ( $\mu_E - \mu_G$ ) values relative to that for (BTDt)<sub>2</sub>ROPh, the solvent spherical cavity sizes for these species are also correspondingly larger.

**Electrochemical Properties.** Figure 5 shows the potentiometrically determined  $E_{1/2}^{0/+}$  and  $E_{1/2}^{-/0}$  values for these proquinoidal D-A-D and A-D-A chromophores; these electrochemical data are tabulated in Table 3. The Figure 5 potentiometric data highlight a number of key electronic structural features of these compounds. For example, replacing ethyne by ethene in the spacer structure [(DHAt)<sub>2</sub>BTD, (DHAd)<sub>2</sub>BTD; (ROPh<sub>t</sub>)<sub>2</sub>TDQ, (ROPh<sub>d</sub>)<sub>2</sub>TDQ] lowers the first oxidation and reduction potentials by  $\sim 350$  and  $\sim 150$  mV, respectively, in these BTD- and TDQ-based chromophores and therefore leads to a correspondingly smaller potentiometrically determined HOMO–LUMO gap ( $E_p$ ), mirroring

**Table 3.** Comparative Potentiometric Data Acquired for Proquinoidal D-A-D and A-D-A Chromophores<sup>a</sup>

	$E_{1/2}^{0/+}$ ( $E_{\text{pa}}$ ) <sup>b</sup>	$E_{1/2}^{-/0}$
(DHAt) <sub>2</sub> BTD	--- (0.40)	−1.74
(DHAd) <sub>2</sub> BTD	0.04 (0.12)	−1.92
(ROPh <sub>t</sub> ) <sub>2</sub> TDQ	0.76 <sup>c</sup> (0.80)	−1.28
(ROPh <sub>d</sub> ) <sub>2</sub> TDQ	--- (0.38)	−1.39
(DHA-BTDt) <sub>2</sub> BTD	--- (0.36)	−1.70
(BTDt) <sub>2</sub> ROPh	0.91 (0.98)	−1.84
(DHAtPh <sub>t</sub> ) <sub>2</sub> ROPh	--- (0.43)	---
	0.46 <sup>d</sup> (0.57)	−2.54 <sup>d</sup>
(DHAtBTDt) <sub>2</sub> ROPh	--- (0.46)	−1.72
	0.36 <sup>c</sup> (0.44)	−1.66 <sup>c</sup>
(DHAtROPh <sub>t</sub> ) <sub>2</sub> BTD	0.32 (0.41)	−1.66

<sup>a</sup> Cyclic voltammetric experimental conditions: [chromophore] =  $\sim 1$  mM; solvent =  $\text{CH}_2\text{Cl}_2$ ; [TBAPF<sub>6</sub>] = 0.10 M; scan rate = 200 mV/s; reference electrode = SCE; working electrode = Pt disk or glassy carbon. All potentials are reported relative to the ferrocene/ferrocenium redox couple, which was used as an internal standard in these experiments. <sup>b</sup> Anodic peak potential. <sup>c</sup> Scan rate = 400 or 500 mV/s. <sup>d</sup> In THF. <sup>e</sup> In PhCN.

the trend observed for the optical band gaps ( $E_{\text{op}}$ ) of these species (Figure 2).

The structures of (DHA-BTDt)<sub>2</sub>BTD and (DHAt)<sub>2</sub>BTD are closely related; (DHA-BTDt)<sub>2</sub>BTD features terminal dihexylamino groups directly attached to benzothiadiazole rather than phenyl groups. Figure 5 data suggest that replacement of the terminal phenyl by BTD destabilizes the HOMO level by 0.04 V, while stabilizing the LUMO to a similar degree; these data thus indicate that (DHA-BTDt)<sub>2</sub>BTD and (DHAt)<sub>2</sub>BTD possess comparable extents of electronic delocalization and ICT character in their respective ground and low energy excited states.

Note that the reduction potential of (BTDt)<sub>2</sub>ROPh (−1.84 V vs  $\text{Fc}/\text{Fc}^+$ ) is shifted cathodically relative to that for 4,7-bis[(trimethylsilyl)ethynyl]benzo[*c*][1,2,5]thiadiazole (BTD(E-TMS)<sub>2</sub>) (−1.66 V). Because the ethyne group typically acts as a weak acceptor, the higher reduction potential of BTD(E-TMS)<sub>2</sub> compared to (BTDt)<sub>2</sub>ROPh suggests that the two terminal benzothiadiazole groups in (BTDt)<sub>2</sub>ROPh are not strongly conjugated to the central dialkoxyphenyl unit in the LUMO level.

Finally, Figure 5 shows that the reduction potential of (DHAtBTDt)<sub>2</sub>ROPh (−1.72 V) is  $\sim 100$  mV stabilized relative to that determined for (BTDt)<sub>2</sub>ROPh, as expected due its expanded conjugation. In contrast, note that the oxidation potential of (DHAtBTDt)<sub>2</sub>ROPh is similar to that of (DHAtPh<sub>t</sub>)<sub>2</sub>ROPh, suggesting that the HOMO is localized extensively on the dihexylaminophenyl groups or only weakly delocalized with the remainder of linear  $\pi$ -conjugated system. Likewise, these potentiometric data indicate that the reduction potential of (DHAtROPh<sub>t</sub>)<sub>2</sub>BTD (−1.66 V) resembles that of BTD(E-TMS)<sub>2</sub>, suggesting a LUMO localized primarily on the diethynylbenzothiadiazole unit; this trend is evident in the Figure 5 data, which shows clearly that the BTD and TDQ units play a dominant role in determining the potentiometrically determined LUMO levels.

**Two-Photon Absorption Spectra.** Two-photon absorption cross sections were determined by measurements of two-photon fluorescence excitation spectra<sup>98,99</sup> with femtosecond laser pulses in the spectral range between 750 and 960 nm. The two-photon



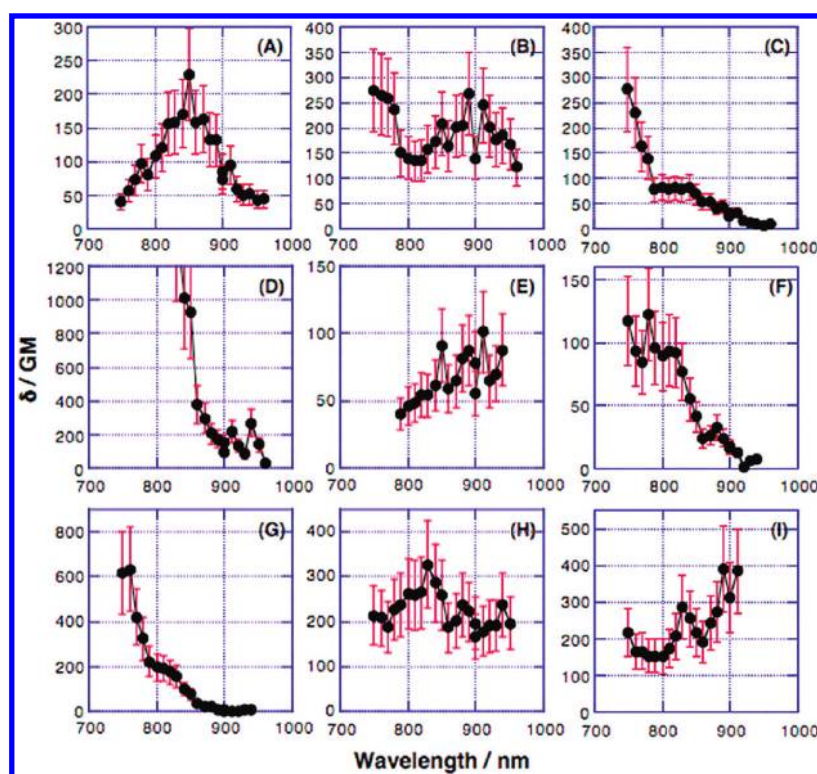
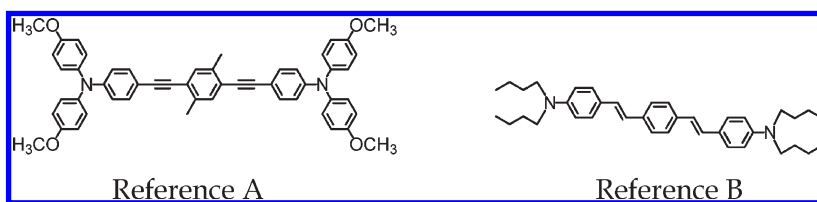


**Figure 6.** Two-photon fluorescence excitation spectra determined in toluene solvent for (A) (DHAt)<sub>2</sub>BTD, (B) (DHAd)<sub>2</sub>BTD, (C) (ROPh)<sub>2</sub>TDQ, (D) (ROPhd)<sub>2</sub>TDQ, (E) (DHA-BTDt)<sub>2</sub>BTD, (F) (BTDt)<sub>2</sub>ROPh, (G) (DHAtPh)<sub>2</sub>ROPh, (H) (DHAtBTDt)<sub>2</sub>ROPh, and (I) (DHAtROPh)<sub>2</sub>BTD. Systematic error for  $\delta$  is  $\pm 30\%$  for each point.

**Table 4.** TPA Data Acquired for Proquinoidal D-A-D and A-D-A Chromophores along with Those for Reference Compounds in Toluene Solvent

	$E_{ge}^a$ (eV)	$\epsilon_{max}^b$ ( $M^{-1} cm^{-1}$ )	$M_{ge}^c$ (D)	TPA maxima (nm)	$\hbar\omega^d$ (eV)	$E_{ge} - \hbar\omega$ (eV)	$\delta^e$ (GM)	$M_{ee}^f$ (D)
(DHAt) <sub>2</sub> BTD	2.47	35300	8.00	850	1.46	1.01	230	6.9
(DHAd) <sub>2</sub> BTD	2.30	37000	8.53	890	1.39	0.91	270	6.5
(ROPh) <sub>2</sub> TDQ	2.21	20400	6.39	<sup>g</sup>	<sup>g</sup>	<sup>g</sup>	<sup>g</sup>	<sup>g</sup>
(ROPhd) <sub>2</sub> TDQ	1.98	20100	6.62	<sup>g</sup>	<sup>g</sup>	<sup>g</sup>	<sup>g</sup>	<sup>g</sup>
(DHA-BTDt) <sub>2</sub> BTD	2.26	46100	9.19	910	1.36	0.90	100	3.7
(BTDt) <sub>2</sub> ROPh	2.92	27700	6.96	780	1.59	1.33	120	6.9
(DHAtPh) <sub>2</sub> ROPh	3.09	94100	12.66	760	1.63	1.46	630	9.2
(DHAtBTDt) <sub>2</sub> ROPh	2.41	69600	11.41	830	1.49	0.92	330	5.1
(DHAtROPh) <sub>2</sub> BTD	2.51	56400	10.30	890	1.39	1.12	390	8.0
reference A <sup>h</sup>	3.19		11.4	712	1.74	1.45	980	12.4
reference B <sup>i</sup>	3.03		10.7	730	1.70	1.33	995	12.1

<sup>a</sup>  $S_0 \rightarrow S_1$  electronic transition. <sup>b</sup> Extinction coefficient. <sup>c</sup>  $S_0 \rightarrow S_1$  transition dipole moment. <sup>d</sup> Excitation energy. <sup>e</sup> Two photon absorption cross section. <sup>f</sup> Transition dipole moment between the  $S_1$  state and two-photon allowed higher-lying excited states. <sup>g</sup> These parameters were not evaluated for TDQ derivatives due to possible mixing of OPA and TPA. <sup>h,i</sup> For the Reference A and B compounds: <sup>h,i</sup> For the Reference A and B compounds, tabulated values were extracted from ref 102<sup>h</sup> and ref 24.<sup>i</sup>



induced fluorescence excitation spectra are shown in Figure 6. TPA cross sections ( $\delta$  values; expressed in Göppert-Mayer or GM units,

where  $1 \text{ GM} = 1 \times 10^{-50} \text{ cm}^4 \text{ s molecule}^{-1} \text{ photon}^{-1}$ ), and maxima, are given in Table 4.

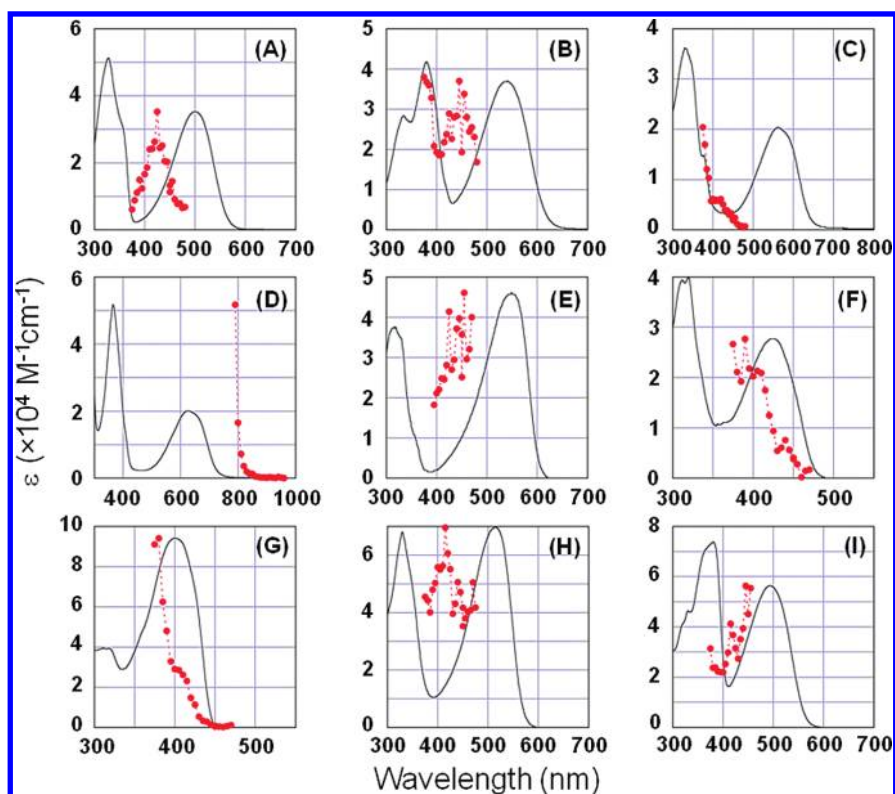


**Figure 7.** Normalized one-photon absorption and two-photon excitation spectra of: (A) (DHAt)<sub>2</sub>BDT, (B) (DHAd)<sub>2</sub>BDT, (C) (ROPh)<sub>2</sub>TDQ, (D) (ROPhd)<sub>2</sub>TDQ, (E) (DHA-BTDt)<sub>2</sub>BDT, (F) (BTDt)<sub>2</sub>ROPh, (G) (DHAtPh)<sub>2</sub>ROPh, (H) (DHAtBTDt)<sub>2</sub>ROPh, and (I) (DHAtROPh)<sub>2</sub>BDT. The solid line represents the one-photon absorption spectrum. The two-photon fluorescence excitation spectral data are displayed as solid circles (the dotted line serves only as a guide to the eye). Except for (ROPhd)<sub>2</sub>TDQ (D), the two-photon fluorescence excitation spectral data are plotted as a function of the total transition energy (twice the photon energy). Note that the (ROPhd)<sub>2</sub>TDQ fluorescence excitation data is plotted as a function of the photon energy to highlight the extent to which the TPA magnitude rises near the low energy absorption edge.

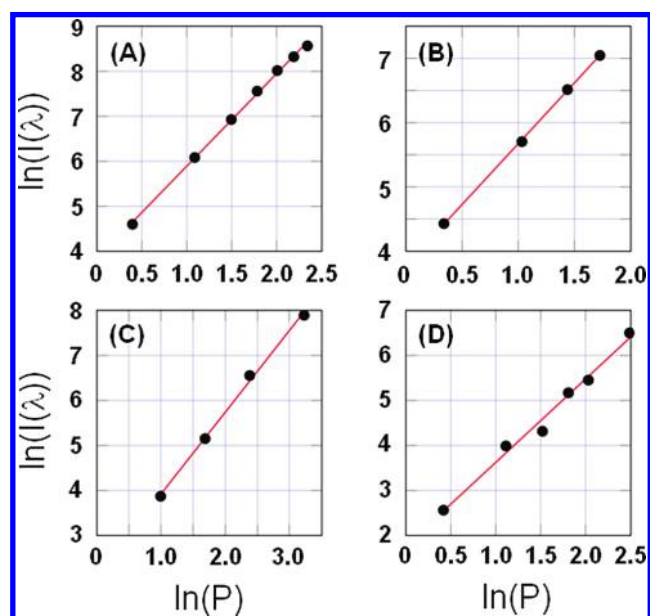


**Figure 8.** Dependence of the two-photon excited fluorescence intensity, plotted logarithmically as a function of the logarithm of the laser power  $P$ , for chromophores (A) (DHAt)<sub>2</sub>BDT, (B) (DHAd)<sub>2</sub>BDT, (C) (ROPh)<sub>2</sub>TDQ, and (D) (DHAtPh)<sub>2</sub>ROPh.

**Table 5.** Linearity Tests for Power-Squared Fluorescence Dependence of Proquinoid D-A-D and A-D-A Chromophores in Toluene Solvent

compounds	$\lambda$ (nm)	slope <sup>a,b</sup>
(DHAt) <sub>2</sub> BDT	850	2.06
(DHAd) <sub>2</sub> BDT	900	1.89
(ROPh) <sub>2</sub> TDQ	780	1.82
(BTDt) <sub>2</sub> ROPh	810	1.65
(DHAtPh) <sub>2</sub> ROPh	830	1.86
(DHAtBTDt) <sub>2</sub> ROPh	870	1.77
(DHAtROPh) <sub>2</sub> BDT	900	2.07

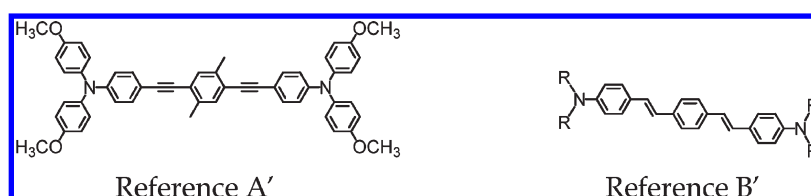
<sup>a</sup> Values displayed are the slopes of the linear regression fits to logarithmic plots of fluorescence intensity versus incident excitation laser intensity. <sup>b</sup> Estimated uncertainty of the slope is  $\pm 0.1$ .

Based on their spectral shapes (Figure 6), the actual TPA peaks of (DHA-BTDt)<sub>2</sub>BDT, (BTDt)<sub>2</sub>ROPh, (DHAtPh)<sub>2</sub>ROPh, and (DHAtROPh)<sub>2</sub>BDT may lie outside of the spectral window analyzed in the present study; otherwise, the peak TPA cross sections for all of the present compounds are comparable to those of similar benzothiadiazole derivatives reported recently.<sup>100,101</sup> To facilitate comparison with the corresponding OPA spectra, TPA spectra are plotted as a

Table 6. Fluorescence Lifetime Data for Proquinoidal D-A-D and A-D-A Chromophores Determined in Toluene Solvent

	$\tau_f$ (ns) <sup>a</sup>	$k_r$ ( $\times 10^7 \text{ s}^{-1}$ )	$k_{nr}$ ( $\times 10^7 \text{ s}^{-1}$ )	$k_r$ (calcd; $\times 10^7 \text{ s}^{-1}$ )
(DHAt) <sub>2</sub> BTd	4.40	19.1	3.63	19.1
(DHAd) <sub>2</sub> BTd	4.71	8.92	12.3	17.6
(ROPh) <sub>2</sub> TDQ	6.63	6.33	8.75	9.68
(ROPhd) <sub>2</sub> TDQ	3.55	0.958	27.2	7.94
(DHA-BTDt) <sub>2</sub> BTd	0.78	11.3	117	23.3
(BTDt) <sub>2</sub> ROPh	3.13	21.1	10.8	23.5
(DHAtPh) <sub>2</sub> ROPh	0.73	122	15.0	109
(DHAtBTDt) <sub>2</sub> ROPh	3.10	25.8	6.46	40.0
(DHAtROPh) <sub>2</sub> BTd	2.80	20.0	15.7	33.0
reference A' <sup>b</sup>	0.74	104	31.1	
reference B' <sup>c</sup>	1.1	84.5	6.4	

<sup>a</sup> The uncertainty of the lifetime measurements was  $\pm 0.05$  ns. <sup>b,c</sup> For the Reference A' and B' compounds, tabulated values were extracted from ref 102<sup>b</sup> and ref 104.<sup>c</sup>



function of  $\lambda_{ex}/2$  (Figure 7). All of the compounds showed TPA maxima higher in energy than the corresponding OPA maxima.

Linearity tests of power-squared fluorescence intensity dependence vs laser power were performed at varying laser excitation wavelengths for selected samples and are shown in Figure 8; the corresponding magnitudes of these slopes are given in Table 5. While the large TPA cross sections below 800 nm for (ROPh)<sub>2</sub>TDQ may arise from residual OPA, it is important to note that the slope (1.82) of the two-photon excited fluorescence intensity as a function of the logarithm of the laser power at 780 nm indicates significant TPA. Note that the available spectral window for (ROPhd)<sub>2</sub>TDQ (Figure 7D) was mostly dominated by OPA; all other compounds showed pure TPA within the spectral window interrogated.

The TPA cross section  $\delta$  is related to the imaginary part of the second-order hyperpolarizability  $\gamma$  through eq 3,<sup>24,28</sup>

$$\delta = \frac{4\pi^2\hbar\omega^2}{n^2c^2}L^4\text{Im}\gamma(-\omega; \omega, -\omega, \omega) \quad (3)$$

where  $\hbar$  is Planck's constant divided by  $2\pi$ ,  $\omega$  is the excitation frequency,  $n$  is the refractive index of the medium,  $c$  is the speed of light,  $L$  is the local field factor ( $L = (n^2 + 2)/3$ ), and  $\text{Im}$  indicates the imaginary part of the complex quantity  $\langle\gamma\rangle$ , the orientational average of  $\gamma$ , i.e.

$$\text{Im}\gamma = \frac{4}{5} \times \text{Im} \left[ \frac{\frac{M_{ge}^2 \times \Delta\mu_{ge}^2}{(E_{ge} - \hbar\omega - i\Gamma_{ge})^2(E_{ge} - 2\hbar\omega - i\Gamma_{ge})}} + \sum_{e'} \frac{\frac{M_{ge}^2 \times M_{ee'}^2}{(E_{ge} - \hbar\omega - i\Gamma_{ge})^2(E_{ge} - 2\hbar\omega - i\Gamma_{ge'})}} - \frac{M_{ge}^4}{(E_{ge} - \hbar\omega - i\Gamma_{ge})^2(E_{ge} + \hbar\omega + i\Gamma_{ge})} \right] \quad (4)$$

Here  $M_{ge}$  is the transition dipole moment between the ground state ( $S_0$ ) and the first excited state ( $S_1$ ),  $\Delta\mu_{ge}$  is the difference in

dipole moments between  $S_0$  and  $S_1$ ,  $E_{ge}$  is the transition energy between  $S_0$  and  $S_1$ ,  $\hbar\omega$  is the excitation energy,  $\Gamma$  is a damping factor, and  $M_{ee'}$  is the transition dipole moment between  $S_1$  and two-photon allowed higher excited states.

The first term in eq 4 is the dipolar term, which is absent for quadrupolar compounds because  $\Delta\mu_{ge}$  vanishes. The third term is related to one-photon resonance and has no contribution to the TPA. Therefore, eq 4 is dominated by the second term for quadrupolar compounds. Despite cancellation of the dipolar term, TPA cross sections of quadrupolar structures have been demonstrated to be higher than those of dipolar analogues; note that the  $M_{ee'}$  term similarly vanishes for corresponding dipolar chromophores.<sup>28</sup> The three-state TPA cross section for quadrupolar compounds with electronic states  $g$ ,  $e$ , and  $e'$  is

$$\delta \approx \frac{16\pi^2(\hbar\omega)^2L^4}{5n^2c^2\hbar} \frac{M_{ge}^2M_{ee'}^2}{(E_{ge} - \hbar\omega)^2\Gamma_{ge'}} \quad (5)$$

The transition moments  $M_{ge}$  are obtained from the area under the lowest energy absorption band. The energy difference ( $E_{ge} - \hbar\omega$ ) is a detuning factor.  $\Gamma_{ge'}$  was assumed to be 0.1 eV in all cases.<sup>22,24,28</sup>  $M_{ee'}$  was derived using eq 5, along with the other experimental parameters. Each parameter of eq 5 is tabulated in Table 4.

As expected from eq 5, the TPA cross section of quadrupolar compounds can be enhanced (within a three-state ansatz) by (i) increasing the transition dipole moment between the ground state and the first excited state, (ii) increasing the transition dipole moment between the first and higher excited states, and (iii) decreasing the detuning factor. Because  $\delta$  is proportional to the square of these quantities, the magnitude of the TPA response can be very sensitive to small changes in electronic structure.

The  $M_{ge}$  values of (DHAt)<sub>2</sub>BTd (8.00 D) and (DHAd)<sub>2</sub>BTd (8.53 D) are slightly smaller than those of the corresponding



**Table 7.** Calculated OPA and TPA Band Maxima and TPA Cross Sections ( $\delta$ ) of Proquinoidal D-A-D and A-D-A Chromophores, Along with Corresponding Experimental Data Obtained in Toluene Solvent<sup>a</sup>

	OPA (calcd) $\lambda$ (nm)	TPA (calcd) $\lambda$ (nm)	$\delta$ (calc) GM	OPA (expt) $\lambda$ (nm)	TPA (expt) $\lambda$ (nm)	$\delta$ (expt) GM
(DHAt) <sub>2</sub> BTd	599	969	504	501	850	230
(DHAd) <sub>2</sub> BTd	633	990	464	540	890	270
(ROPh) <sub>2</sub> TDQ	679	966	487	562	<sup>b</sup>	<sup>b</sup>
(ROPhd) <sub>2</sub> TDQ	772	1,033	598	626	<sup>b</sup>	<sup>b</sup>
(DHA-BTDt) <sub>2</sub> BTd	608	981	652	549	910	100
(BTDt) <sub>2</sub> ROPh	523	992	114	424	780	120
(DHAtPh) <sub>2</sub> ROPh	430	783	1308	401	760	630
(DHAtBTDt) <sub>2</sub> ROPh	633	1093	1725	515	830	330
(DHAtROPh) <sub>2</sub> BTd	659	1181	1200	494	890	390

<sup>a</sup> Computational values were determined for vacuum. <sup>b</sup> These parameters were not evaluated for TDQ derivatives due to possible mixing of OPA and TPA.

reference compounds (11.4 and 10.7 D, respectively, for 1,4-bis[(4'-N,N-bis(4''-methoxyphenyl)aminophenyl)ethyn-1'-yl]-2,5-dimethylbenzene (reference A in Table 4)<sup>102</sup> and 1,4-bis[(4'-N,N-dibutylaminophenyl)ethen-1'-yl]benzene (reference B in Table 4),<sup>24</sup> in which the BTd moiety is replaced by phenyl. As the radiative rate constant ( $k_r$ ) is proportional to the square of  $M_{ge}$ ,<sup>103</sup> these proquinoidal D-A-D and A-D-A molecules manifest diminished  $k_r$  values with respect to these phenylene-based reference compounds (Table 6).<sup>102,104</sup> Radiative rate constants were determined from the fluorescence quantum yields and fluorescence lifetimes using

$$\Phi_f = \frac{k_r}{k_r + k_{nr}} \quad (6)$$

$$\tau_f = \frac{1}{k_r + k_{nr}} \quad (7)$$

In these equations,  $\Phi_f$  is the fluorescence quantum yield,  $k_r$  and  $k_{nr}$  are radiative and nonradiative rate constants, respectively, and  $\tau_f$  is the fluorescence lifetime. Radiative rate constants for these chromophores were also estimated from the Strickler–Berg relation and their corresponding absorption and fluorescence spectra.<sup>103</sup> The experimental and calculated radiative rate constants matched well for these BTd- and TDQ-based chromophores, and are smaller than those determined previously for their corresponding phenylene-based reference compounds (see Table 6 references). Note as well that the detuning factors of these proquinoidal chromophores are smaller than those determined previously for their respective corresponding reference compounds (Table 4), in which the BTd and TDQ units are replaced by simple aryl structures. Because smaller detuning factors increase TPA cross sections, measured decreases of TPA cross sections in these proquinoidal chromophores relative to their respective phenylene analogues would therefore be expected to derive from smaller  $M_{ge}$  values for these species, consistent with the data in Table 4. Note that (DHAtBTDt)<sub>2</sub>ROPh and (DHAtROPh)<sub>2</sub>BTd, which have extended  $\pi$ -conjugated structures relative to (DHAt)<sub>2</sub>BTd, evince higher TPA cross sections, suggesting that increased conjugation length is an important factor to enhance TPA, consistent with other reports.<sup>24,32,105</sup>

## THEORETICAL ANALYSIS

To provide further insight into the origins of the OPA and TPA properties of these proquinoidal D-A-D and A-D-A

quadrupolar chromophores, the one- and two-photon absorption spectra for these species were computed. Each structure was simplified and optimized using HF/6-31G methods for structures with  $\pi$ -systems constrained to remain planar; time-dependent density-functional theory (TDDFT) with the collective electronic oscillator (CEO) framework<sup>86</sup> was used to compute the one- and two-photon absorption spectra for these structures (see Experimental Section). Data obtained from these calculations are tabulated in Table 7.

For OPA, these TDDFT calculations provided qualitative agreement with experimental excitation frequencies and transition intensities. Note that the calculated frequencies of the lowest energy excitations are red-shifted by  $\sim 100$ – $200$  nm (about 0.2–0.6 eV) relative to that determined by experiment for all of the molecules studied. Such transition energy discrepancies between theory and experiment have been noted previously<sup>86</sup> and have been ascribed to several sources; these include (1) solute–solvent interactions, not accounted for computationally, that lead to geometrical distortions and shortening of the effective conjugation length or localization of charge and (2) the fact that the TDDFT approach overestimates the extent of exciton delocalization.<sup>106,107</sup>

For TPA spectra, the simulations revealed that compounds with increased conjugation length (e.g., (DHAtPh)<sub>2</sub>ROPh, (DHAtBTDt)<sub>2</sub>ROPh, and (DHAtROPh)<sub>2</sub>BTd) relative to (DHAt)<sub>2</sub>BTd exhibit stronger TPA, consistent with experiment. Note that these calculated cross sections are about 2–5 times larger than the experimental values. Such overestimation of calculated TPA cross sections relative to those determined experimentally is a common artifact of this computational approach and can be ascribed to several factors. Foremost, the conventional exchange–correlation functionals employed in these simulations often fail to effectively describe charge transfer.<sup>89,108,109</sup> Further, the molecular structures were optimized using symmetry constraints described above; this simplification neglects the rotational degrees of freedom between the donor and acceptor units of these chromophores and access to other lower symmetry species in the ensemble. To test this hypothesis, we calculated TPA spectra for nonplanar (DHAt)<sub>2</sub>BTd structures. In this set of simulations, the dihedral angles between the phenylene and BTd ring systems were varied, and TPA spectra were calculated for multiple combinations of twist angles (data not shown). These studies found that the calculated TPA values were strongly

influenced by the planarity of the structure, and that the absorption cross section decreased dramatically with the increasing twist-angle magnitude; the calculated minimum TPA cross section was found to be less than one-fifth of the maximum cross-sectional value determined for the planar structure.

The agreement between calculation and experiment was closest for (DHAt)<sub>2</sub>BTD, (DHAd)<sub>2</sub>BTD, and (DHAtPht)<sub>2</sub>ROPh, which evinced a factor of 2 difference between the measured and computed TPA cross sections and computed red-shifts of the lowest absorption maxima within 100 nm of the respective experimental values. The discrepancy between measured and computed values of  $\delta$  and the TPA band maximum was larger for the more conjugated (DHAtBTDt)<sub>2</sub>ROPh and (DHAtROPht)<sub>2</sub>BTD chromophores; this result is consistent with the expectation that these species likely access a range of structures having varying degrees of conjugation in solution. The calculated  $\delta$  values for (DHAtPht)<sub>2</sub>ROPh, (DHAtBTDt)<sub>2</sub>ROPh, and (DHAtROPht)<sub>2</sub>BTD exceed those computed for (DHAt)<sub>2</sub>BTD, consistent both with experiment and the expectation that increasing conjugation length in these proquinoidal quadrupolar chromophores is an important contributor to enhance TPA cross section.

## CONCLUSION

$\pi$ -Conjugated proquinoidal quadrupolar chromophores that feature either donor–acceptor–donor (D-A-D) or acceptor–donor–acceptor (A-D-A) electronic motifs and utilize benzo-[c][1,2,5]thiadiazole (BTD) or 6,7-bis(3',7'-dimethyloctyl)[1,2,5]-thiadiazolo[3,4-g]quinoxaline (TDQ) electron acceptor units were designed and synthesized. The lowest energy absorption bands of these proquinoidal compounds are red-shifted  $\sim 100$  nm relative to the transitions of corresponding reference chromophores that incorporate phenylene components in place of BTD and TDQ moieties. These chromophores exhibit large fluorescence spectral red-shifts and concomitant decreases of fluorescence quantum yield with increasing solvent polarity, indicating that these species possess relaxed singlet excited states having significant internal charge transfer (ICT) character. These proquinoidal species manifest blue-shifted two-photon absorption spectra relative to their corresponding one-photon absorption spectrum and display high TPA cross sections ( $>100$  GM) within these spectral windows. D-A-D and A-D-A structures within this series that feature more extensive conjugation exhibit larger TPA cross sections; theoretical analysis of these spectral properties are consistent with this trend. Two proquinoidal quadrupolar chromophores, (DHAtBTDt)<sub>2</sub>ROPh and (DHAtROPht)<sub>2</sub>BTD, showed TPA cross sections over 150 GM in the spectral region between 750 and 960 nm. This optical excitation window is easily achieved with a mode-locked femtosecond titanium-sapphire laser, which is most frequently used for two-photon-excited fluorescence imaging. Proquinoidal D-A-D and A-D-A chromophores that feature BTD components manifest high fluorescence quantum yields ( $0.6 < \Phi_f < 0.9$ ) in environments with low solvent polarity. This property makes these species attractive as dopants in nanoscale matrices, such as polymersomes,<sup>110–112</sup> as the combination of large TPA cross section and substantial fluorescence emission provides added imaging utility. Additionally, because the nonlinear properties of dipolar and quadrupolar compounds are governed by different parameters, such D-A-D and A-D-A chromophores complement the

orthogonal imaging utility of D–A structures in applications such as second harmonic generation imaging.<sup>113–115</sup>

## ASSOCIATED CONTENT

**S Supporting Information.** Detailed synthetic procedures; tabulated absorption and fluorescence data. This material is available free of charge via the Internet at <http://pubs.acs.org>.

## AUTHOR INFORMATION

### Corresponding Author

E-mail: david.beratan@duke.edu (D.N.B.), yodh@physics.upenn.edu (A.G.Y.), and michael.therien@duke.edu (M.J.T.).

### Present Addresses

\*Optical Sciences Division, Naval Research Laboratory, Washington, DC 20375.

<sup>†</sup>Laboratory of Sensory Neuroscience, The Rockefeller University, New York City, NY 10065.

## ACKNOWLEDGMENT

The authors thank Professor Felix N. Castellano and Dr. Radiy Islangulov for their assistance with fluorescence lifetime measurements. D.N.B. is grateful to Dr. Sergei Tretiak for providing the CEO program and to Professor Artëm Masunov and Dr. Xiangqian Hu for helpful discussion. The authors thank the Department of Energy (DE-SC0001517), the National Institutes of Health (RO1GM48043) and the MRSEC Program of the National Science Foundation (DMR0520020) for supporting this work; J.A.N.F. is grateful to Bristol-Myers Squibb for a Basic Neurosciences Postdoctoral Fellowship. D.N.B. thanks the National Science Foundation (CHE-1012357) for support.

## REFERENCES

- (1) Parthenopoulos, D. A.; Rentzepis, P. M. *Science* **1989**, *245*, 843–845.
- (2) Strickler, J. H.; Webb, W. W. *Adv. Mater.* **1993**, *5*, 479–481.
- (3) Dvornikov, A. S.; Walker, E. P.; Rentzepis, P. M. *J. Phys. Chem. A* **2009**, *113*, 13633–13644.
- (4) Zhou, W.; Kuebler, S. M.; Braun, K. L.; Yu, T.; Cammack, J. K.; Ober, C. K.; Perry, J. W.; Marder, S. R. *Science* **2002**, *296*, 1106–1109.
- (5) Pruzinsky, S. A.; Braun, P. V. *Adv. Funct. Mater.* **2005**, *15*, 1995–2004.
- (6) Lee, K. S.; Yang, D. Y.; Park, S. H.; Kim, R. H. *Polym. Adv. Technol.* **2006**, *17*, 72–82.
- (7) Denk, W.; Strickler, J. H.; Webb, W. W. *Science* **1990**, *248*, 73–76.
- (8) Xu, C.; Zipfel, W.; Shear, J. B.; Williams, R. M.; Webb, W. W. *Proc. Natl. Acad. Sci. U.S.A.* **1996**, *93*, 10763–10768.
- (9) Cahalan, M. D.; Parker, I.; Wei, S. H.; Miller, M. J. *Nat. Rev. Immun.* **2002**, *2*, 872–880.
- (10) Zipfel, W. R.; Williams, R. M.; Webb, W. W. *Nat. Biotechnol.* **2003**, *21*, 1368–1376.
- (11) Krishna, T. R.; Parent, M.; Werts, M. H. V.; Moreaux, L.; Gmouh, S.; Charpak, S.; Caminade, A. M.; Majoral, J. P.; Blanchard-Desce, M. *Angew. Chem., Int. Ed.* **2006**, *45*, 4645–4648.
- (12) Zheng, Q. D.; Xu, G. X.; Prasad, P. N. *Chem.—Eur. J.* **2008**, *14*, 5812–5819.
- (13) Spangler, C. W. *J. Mater. Chem.* **1999**, *9*, 2013–2020.
- (14) Oliveira, S. L.; Corrêa, D. S.; Misoguti, L.; Constantino, C. J. L.; Aroca, R. F.; Zilio, S. C.; Mendonça, C. R. *Adv. Mater.* **2005**, *17*, 1890–1893.
- (15) Charlot, M.; Izard, N.; Mongin, O.; Riehl, D.; Blanchard-Desce, M. *Chem. Phys. Lett.* **2006**, *417*, 297–302.

- (16) Zheng, Q. D.; Gupta, S. K.; He, G. S.; Tan, L. S.; Prasad, P. A. N. *Adv. Funct. Mater.* **2008**, *18*, 2770–2779.
- (17) Frederiksen, P. K.; Jørgensen, M.; Ogilby, P. R. *J. Am. Chem. Soc.* **2001**, *123*, 1215–1221.
- (18) Liu, J.; Zhao, Y. W.; Zhao, J. Q.; Xia, A. D.; Jiang, L. J.; Wu, S.; Ma, L.; Dong, Y. Q.; Gu, Y. H. *J. Photochem. Photobiol. B* **2002**, *68*, 156–164.
- (19) McIlroy, S. P.; Clo, E.; Nikolajsen, L.; Frederiksen, P. K.; Nielsen, C. B.; Mikkelsen, K. V.; Gothelf, K. V.; Ogilby, P. R. *J. Org. Chem.* **2005**, *70*, 1134–1146.
- (20) Oar, M. A.; Serin, J. A.; Dichtel, W. R.; Frechet, J. M. J. *Chem. Mater.* **2005**, *17*, 2267–2275.
- (21) Beverina, L.; Crippa, M.; Landenna, M.; Ruffo, R.; Salice, P.; Silvestri, F.; Versari, S.; Villa, A.; Ciaffoni, L.; Collini, E.; Ferrante, C.; Bradamante, S.; Mari, C. M.; Bozio, R.; Pagani, G. A. *J. Am. Chem. Soc.* **2008**, *130*, 1894–1902.
- (22) Albota, M.; Beljonne, D.; Brédas, J.-L.; Ehrlich, J. E.; Fu, J.-Y.; Heikal, A. A.; Hess, S. E.; Kogej, T.; Levin, M. D.; Marder, S. R.; McCord-Maughon, D.; Perry, J. W.; Röckel, H.; Rumi, M.; Subramaniam, G.; Webb, W. W.; Wu, X.-L.; Xu, C. *Science* **1998**, *281*, 1653–1656.
- (23) Ventelon, L.; Moreaux, L.; Mertz, J.; Blanchard-Desce, M. *Chem. Commun.* **1999**, 2055–2056.
- (24) Rumi, M.; Ehrlich, J. E.; Heikal, A. A.; Perry, J. W.; Barlow, S.; Hu, Z.; McCord-Maughon, D.; Parker, T. C.; Röckel, H.; Thayumanavan, S.; Marder, S. R.; Beljonne, D.; Brédas, J.-L. *J. Am. Chem. Soc.* **2000**, *122*, 9500–9510.
- (25) Ventelon, L.; Charier, S.; Moreaux, L.; Mertz, J.; Blanchard-Desce, M. *Angew. Chem., Int. Ed.* **2001**, *40*, 2098–2101.
- (26) Pond, S. J. K.; Rumi, M.; Levin, M. D.; Parker, T. C.; Beljonne, D.; Day, M. W.; Brédas, J.-L.; Marder, S. R.; Perry, J. W. *J. Phys. Chem. A* **2002**, *106*, 11470–11480.
- (27) Iwase, Y.; Kamada, K.; Ohta, K.; Kondo, K. *J. Mater. Chem.* **2003**, *13*, 1575–1581.
- (28) Strehmel, B.; Sarker, A. M.; Detert, H. *ChemPhysChem* **2003**, *4*, 249–259.
- (29) Yang, W. J.; Kim, C. H.; Jeong, M.-Y.; Lee, S. K.; Piao, M. J.; Jeon, S.-J.; Cho, B. R. *Chem. Mater.* **2004**, *16*, 2783–2789.
- (30) Belfield, K. D.; Morales, A. R.; Kang, B.-S.; Hales, J. M.; Hagan, D. J.; Van Stryland, E. W.; Chapela, V. M.; Percino, J. *Chem. Mater.* **2004**, *16*, 4634–4641.
- (31) Yang, W. J.; Kim, D. Y.; Jeong, M.-Y.; Kim, H. M.; Lee, Y. K.; Fang, X.; Jeon, S.-J.; Cho, B. R. *Chem.—Eur. J.* **2005**, *11*, 4191–4198.
- (32) Chung, S.-J.; Rumi, M.; Alain, V.; Barlow, S.; Perry, J. W.; Marder, S. R. *J. Am. Chem. Soc.* **2005**, *127*, 10844–10845.
- (33) Terenziani, F.; Katan, C.; Badaeva, E.; Tretiak, S.; Blanchard-Desce, M. *Adv. Mater.* **2008**, *20*, 4641–4678.
- (34) Kim, H. M.; Cho, B. R. *Chem. Commun.* **2009**, 153–164.
- (35) Barzoukas, M.; Blanchard-Desce, M. *J. Chem. Phys.* **2000**, *113*, 3951–3959.
- (36) Barzoukas, M.; Blanchard-Desce, M. *Proc. SPIE* **2001**, *4461*, 78–89.
- (37) Cho, B. R.; Son, K. H.; Lee, S. H.; Song, Y.-S.; Lee, Y.-K.; Jeon, S.-J.; Choi, J. H.; Lee, H.; Cho, M. *J. Am. Chem. Soc.* **2001**, *123*, 10039–10045.
- (38) Beljonne, D.; Wenseleers, W.; Zojer, E.; Shuai, Z.; Vogel, H.; Pond, S. J. K.; Perry, J. W.; Marder, S. R.; Brédas, J.-L. *Adv. Funct. Mater.* **2002**, *12*, 631–641.
- (39) Le Droumaguet, C.; Mongin, O.; Werts, M. H. V.; Blanchard-Desce, M. *Chem. Commun.* **2005**, 2802–2804.
- (40) Bhaskar, A.; Ramakrishna, G.; Lu, Z. K.; Twieg, R.; Hales, J. M.; Hagan, D. J.; Van Stryland, E.; Goodson, T. *J. Am. Chem. Soc.* **2006**, *128*, 11840–11849.
- (41) Terenziani, F.; Le Droumaguet, C.; Katan, C.; Mongin, O.; Blanchard-Desce, M. *ChemPhysChem* **2007**, *8*, 723–734.
- (42) Collings, J. C.; Poon, S. Y.; Le Droumaguet, C.; Charlot, M.; Katan, C.; Pålsson, L. O.; Beeby, A.; Mosely, J. A.; Kaiser, H. M.; Kaufmann, D.; Wong, W. Y.; Blanchard-Desce, M.; Marder, T. B. *Chem.—Eur. J.* **2009**, *15*, 198–208.
- (43) Chung, S.-J.; Kim, K.-S.; Lin, T.-C.; He, G. S.; Swiatkiewicz, J.; Prasad, P. N. *J. Phys. Chem. B* **1999**, *103*, 10741–10745.
- (44) Katan, C.; Terenziani, F.; Mongin, O.; Werts, M. H. V.; Porrés, L.; Pons, T.; Mertz, J.; Tretiak, S.; Blanchard-Desce, M. *J. Phys. Chem. A* **2005**, *109*, 3024–3037.
- (45) Drobizhev, M.; Karotki, A.; Rebane, A.; Spangler, C. W. *Opt. Lett.* **2001**, *26*, 1081–1083.
- (46) Wei, P.; Bi, X. D.; Wu, Z.; Xu, Z. *Org. Lett.* **2005**, *7*, 3199–3202.
- (47) Varnavski, O.; Yan, X. Z.; Mongin, O.; Blanchard-Desce, M.; Goodson, T. *J. Phys. Chem. C* **2007**, *111*, 149–162.
- (48) Ramakrishna, G.; Bhaskar, A.; Bauerle, P.; Goodson, T. *J. Phys. Chem. A* **2008**, *112*, 2018–2026.
- (49) Kitamura, C.; Tanaka, S.; Yamashita, Y. *Chem. Mater.* **1996**, *8*, 570–578.
- (50) van Mullekom, H. A. M.; Vekemans, J. A. J. M.; Meijer, E. W. *Chem.—Eur. J.* **1998**, *4*, 1235–1243.
- (51) Raimundo, J.-M.; Blanchard, P.; Brisset, H.; Akoudad, S.; Roncali, J. *Chem. Commun.* **2000**, 939–940.
- (52) Morikita, T.; Yamaguchi, I.; Yamamoto, T. *Adv. Mater.* **2001**, *13*, 1862–1864.
- (53) Bangcuyo, C. G.; Evans, U.; Myrick, M. L.; Bunz, U. H. F. *Macromolecules* **2001**, *34*, 7592–7594.
- (54) Justin Thomas, K. R.; Lin, J. T.; Velusamy, M.; Tao, Y.-T.; Chuen, C.-H. *Adv. Funct. Mater.* **2004**, *14*, 83–90.
- (55) Chen, M.; Perzon, E.; Andersson, M. R.; Marcinkevicius, S.; Jönsson, S. K. M.; Fahlman, M.; Berggren, M. *Appl. Phys. Lett.* **2004**, *84*, 3570–3572.
- (56) Susumu, K.; Duncan, T. V.; Therien, M. J. *J. Am. Chem. Soc.* **2005**, *127*, 5186–5195.
- (57) Pai, C. L.; Liu, C. L.; Chen, W. C.; Jenekhe, S. A. *Polymer* **2006**, *47*, 699–708.
- (58) Bundgaard, E.; Krebs, F. C. *Macromolecules* **2006**, *39*, 2823–2831.
- (59) Chen, M. X.; Perzon, E.; Robisson, N.; Joensson, S. K. M.; Andersson, M. R.; Fahlman, M.; Berggren, M. *Synth. Met.* **2004**, *146*, 233–236.
- (60) Yang, R. Q.; Tian, R. Y.; Yan, J. G.; Zhang, Y.; Yang, J.; Hou, Q.; Yang, W.; Zhang, C.; Cao, Y. *Macromolecules* **2005**, *38*, 244–253.
- (61) Chuang, C. Y.; Shih, P. I.; Chien, C. H.; Wu, F. I.; Shu, C. F. *Macromolecules* **2007**, *40*, 247–252.
- (62) Liu, J.; Guo, X.; Bu, L. J.; Xie, Z. Y.; Cheng, Y. X.; Geng, Y. H.; Wang, L. X.; Jing, X. B.; Wang, F. S. *Adv. Funct. Mater.* **2007**, *17*, 1917–1925.
- (63) Qian, G.; Zhong, Z.; Luo, M.; Yu, D.; Zhang, Z.; Ma, D.; Wang, Z. Y. *J. Phys. Chem. C* **2009**, *113*, 1589–1595.
- (64) Velusamy, M.; Justin Thomas, K. R.; Lin, J. T.; Hsu, Y.-C.; Ho, K.-C. *Org. Lett.* **2005**, *7*, 1899–1902.
- (65) Perzon, E.; Wang, X.; Zhang, F.; Mammo, W.; Delgado, J. L.; de la Cruz, P.; Inganäs, O.; Langa, F.; Andersson, M. R. *Synth. Met.* **2005**, *154*, 53–56.
- (66) Wang, X.; Perzon, E.; Mammo, W.; Oswald, F.; Admassie, S.; Persson, N.-K.; Langa, F.; Andersson, M. R.; Inganäs, O. *Thin Solid Films* **2006**, *511–512*, 576–580.
- (67) Zhu, Z.; Waller, D.; Morana, M.; Muhlbacher, D.; Scharber, M.; Brabec, C. *Macromolecules* **2007**, *40*, 1981–1986.
- (68) Shin, W. S.; Kim, S. C.; Lee, S. J.; Jeon, H. S.; Kim, M. K.; Naidu, B. V. K.; Jin, S. H.; Lee, J. K.; Lee, J. W.; Gal, Y. S. *J. Polym. Sci., Part A: Polym. Chem.* **2007**, *45*, 1394–1402.
- (69) McNeill, C. R.; Abruci, A.; Zaumseil, J.; Wilson, R.; McKiernan, M. J.; Burroughes, J. H.; Halls, J. J. M.; Greenham, N. C.; Friend, R. H. *Appl. Phys. Lett.* **2007**, *90*, 193506.
- (70) Bundgaard, E.; Krebs, F. C. *Sol. Energy Mater. Sol. Cells* **2007**, *91*, 1019–1025.
- (71) Sun, M. L.; Wang, L.; Zhu, X. H.; Du, B.; Liu, R.; Yang, W.; Cao, Y. *Sol. Energy Mater. Sol. Cells* **2007**, *91*, 1681–1687.
- (72) Hou, J. H.; Chen, H. Y.; Zhang, S. Q.; Li, G.; Yang, Y. *J. Am. Chem. Soc.* **2008**, *130*, 16144–16145.
- (73) Zoombelt, A. P.; Fonrodona, M.; Wienk, M. M.; Sieval, A. B.; Hummelen, J. C.; Janssen, R. A. J. *Org. Lett.* **2009**, *11*, 903–906.



- (74) Zaumseil, J.; Donley, C. L.; Kim, J.-S.; Friend, R. H.; Sirringhaus, H. *Adv. Mater.* **2006**, *18*, 2708–2712.
- (75) Chen, M.; Crispin, X.; Perzon, E.; Andersson, M. R.; Pullerits, T.; Andersson, M.; Inganäs, O.; Berggren, M. *Appl. Phys. Lett.* **2005**, *87*, 252105.
- (76) Zhang, M.; Tsao, H. N.; Pisula, W.; Yang, C. D.; Mishra, A. K.; Mullen, K. J. *Am. Chem. Soc.* **2007**, *129*, 3472–3473.
- (77) Pilgram, K.; Zupan, M.; Skiles, R. J. *Heterocycl. Chem.* **1970**, *7*, 629–633.
- (78) Tsubata, Y.; Suzuki, T.; Yamashita, Y.; Mukai, T.; Miyashi, T. *Heterocycles* **1992**, *33*, 337–348.
- (79) Therien, M. J.; Susumu, K. PCT Int. Appl. WO 2007/081991 A2, 2007.
- (80) Demas, J. N.; Crosby, G. A. *J. Phys. Chem.* **1971**, *75*, 991–1024.
- (81) Karstens, T.; Kobs, K. *J. Phys. Chem.* **1980**, *84*, 1871–1872.
- (82) Tyson, D. S.; Luman, C. R.; Zhou, X.; Castellano, F. N. *Inorg. Chem.* **2001**, *40*, 4063–4071.
- (83) Luman, C. R. L.; Castellano, F. N. *Photochem. Photobiol.* **2003**, *77*, 510–514.
- (84) Fisher, J. A. N.; Salzberg, B. M.; Yodh, A. G. *J. Neurosci. Meth.* **2005**, *148*, 94–102.
- (85) Fisher, J. A. N.; Susumu, K.; Therien, M. J.; Yodh, A. G. *J. Chem. Phys.* **2009**, *130*, 134506.
- (86) Masunov, A.; Tretiak, S. *J. Phys. Chem. B* **2004**, *108*, 899–907.
- (87) Tretiak, S.; Chernyak, V. *J. Chem. Phys.* **2003**, *119*, 8809–8823.
- (88) Day, P. N.; Nguyen, K. A.; Pachter, R. *J. Phys. Chem. B* **2005**, *109*, 1803–1814.
- (89) Bartholomew, G. P.; Rumi, M.; Pond, S. J. K.; Perry, J. W.; Tretiak, S.; Bazan, G. C. *J. Am. Chem. Soc.* **2004**, *126*, 11529–11542.
- (90) Fabian, J.; Diaz, L. A.; Seifert, G.; Niehaus, T. *THEOCHEM* **2002**, *594*, 41–53.
- (91) Andreu, R.; Garín, J.; Orduna, J. *Tetrahedron* **2001**, *37*, 7883–7892.
- (92) Frisch, M. J.; Trucks, G. W.; Schlegel, H. B.; Scuseria, G. E.; Robb, M. A.; Cheeseman, J. R.; Zakrzewski, V. G.; Montgomery, J. A.; Stratmann, R. E.; Burant, J. C.; Dapprich, S.; Millam, J. M.; Daniels, A. D.; Kudin, K. N.; Strain, M. C.; Farkas, O.; Tomasi, J.; Barone, V.; Cossi, M.; Cammi, R.; Mennucci, B.; Pomelli, C.; Adamo, C.; Clifford, S.; Ochterski, J.; Petersson, G. A.; Ayala, P. Y.; Cui, Q.; Morokuma, K.; Malick, D. K.; Rabuck, A. D.; Raghavachari, K.; Foresman, J. B.; Cioslowski, J.; Ortiz, J. V.; Stefanov, B. B.; Liu, G.; Liashenko, A.; Piskorz, P.; Komaromi, I.; Gomperts, R.; Martin, R. L.; Fox, D. J.; Keith, T.; Al-Laham, M. A.; Peng, C. Y.; Nanayakkara, A.; Gonzalez, C.; Challacombe, M.; Gill, P. M. W.; Johnson, B. G.; Chen, W.; Wong, M. W.; Andres, J. L.; Head-Gordon, M.; Replogle, E. S.; Pople, J. A. *Gaussian 98*, Revision A.9; Gaussian, Inc: Pittsburgh, PA, 1998.
- (93) Tretiak, S.; Mukamel, S. *Chem. Rev.* **2002**, *102*, 3171–3212.
- (94) van Mullekom, H. A. M.; Vekemans, J. A. J. M.; Havinga, E. E.; Meijer, E. W. *Mater. Sci. Eng.* **2001**, *32*, 1–40.
- (95) Nguyen, P.; Yuan, Z.; Agocs, L.; Lesley, G.; Marder, T. B. *Inorg. Chim. Acta* **1994**, *220*, 289–296.
- (96) Ndayikengurukiye, H.; Jacobs, S.; Tachelet, W.; Van Der Looy, J.; Pollaris, A.; Geise, H. J.; Claeys, M.; Kauffmann, J. M.; Janietz, S. *Tetrahedron* **1997**, *53*, 13811–13828.
- (97) Woo, H. Y.; Liu, B.; Kohler, B.; Korystov, D.; Mikhailovsky, A.; Bazan, G. C. *J. Am. Chem. Soc.* **2005**, *127*, 14721–14729.
- (98) Xu, C.; Webb, W. W. *J. Opt. Soc. Am. B* **1996**, *13*, 481–491.
- (99) Albota, M. A.; Xu, C.; Webb, W. W. *Appl. Opt.* **1998**, *37*, 7352–7356.
- (100) Kato, S.-i.; Matsumoto, T.; Ishi-i, T.; Thiemann, T.; Shigeiwa, M.; Gorohmaru, H.; Maeda, S.; Yamashita, Y.; Mataka, S. *Chem. Commun.* **2004**, 2342–2343.
- (101) Kato, S.-i.; Matsumoto, T.; Shigeiwa, M.; Gorohmaru, H.; Maeda, S.; Ishi-i, T.; Mataka, S. *Chem.—Eur. J.* **2006**, *12*, 2303–2317.
- (102) Strehmel, B.; Amthor, S.; Schelter, J.; Lambert, C. *ChemPhysChem* **2005**, *6*, 893–896.
- (103) Strickler, S. J.; Berg, R. A. *J. Chem. Phys.* **1962**, *37*, 814–822.
- (104) Hong, J. W.; Woo, H. Y.; Liu, B.; Bazan, G. C. *J. Am. Chem. Soc.* **2005**, *127*, 7435–7443.
- (105) Najechalski, P.; Morel, Y.; Stéphan, O.; Baldeck, P. L. *Chem. Phys. Lett.* **2001**, *343*, 44–48.
- (106) Grimme, S.; Parac, M. *ChemPhysChem* **2003**, *4*, 292–295.
- (107) Cai, Z.-L.; Sendt, K.; Reimers, J. R. *J. Chem. Phys.* **2002**, *117*, 5543–5549.
- (108) Tozer, D. J.; Amos, R. D.; Handy, N. C.; Roos, B. O.; Serrano-Andres, L. *Mol. Phys.* **1999**, *97*, 859–868.
- (109) Neiss, C.; Saalfrank, P.; Parac, M.; Grimme, S. *J. Phys. Chem. A* **2003**, *107*, 140–147.
- (110) Ghoroghchian, P. P.; Frail, P. R.; Susumu, K.; Blessington, D.; Brannan, A. K.; Bates, F. S.; Chance, B.; Hammer, D. A.; Therien, M. J. *Proc. Natl. Acad. Sci. U.S.A.* **2005**, *102*, 2922–2927.
- (111) Ghoroghchian, P. P.; Frail, P. R.; Susumu, K.; Park, T.-H.; Wu, S. P.; Uyeda, H. T.; Hammer, D. A.; Therien, M. J. *J. Am. Chem. Soc.* **2005**, *127*, 15388–15390.
- (112) Ghoroghchian, P. P.; Frail, P. R.; Li, G.; Zupancich, J. A.; Bates, F. S.; Hammer, D. A.; Therien, M. J. *Chem. Mater.* **2007**, *19*, 1309–1318.
- (113) Moreaux, L.; Sandre, O.; Blanchard-Desce, M.; Mertz, J. *Opt. Lett.* **2000**, *25*, 320–322.
- (114) Reeve, J. E.; Collins, H. A.; De Mey, K.; Kohl, M. M.; Thorley, K. J.; Paulsen, O.; Clays, K.; Anderson, H. L. *J. Am. Chem. Soc.* **2009**, *131*, 2758–2759.
- (115) Therien, M. J. *Nature* **2009**, *458*, 716–717.